UNIVERSIDADE DE LISBOA
FACULDADE DE CIÊNCIAS
DEPARTAMENTO DE BIOLOGIA VEGETAL

Production of lipids (for biodiesel) and carotenoids from the yeast *Rhodotorula glutinis* grown in a bench reactor, in a fed-batch system

João Pedro Rascão Ascensão Caldeira

Dissertação
Mestrado em Microbiologia Aplicada

2015

UNIVERSIDADE DE LISBOA
FACULDADE DE CIÊNCIAS
DEPARTAMENTO DE BIOLOGIA VEGETAL

Production of lipids (for biodiesel) and carotenoids from the yeast *Rhodotorula glutinis* grown in a bench reactor, in a fed-batch system

João Pedro Rascão Ascensão Caldeira

Dissertação
Mestrado em Microbiologia Aplicada

Orientadores
Externo: Doutora Maria Teresa Saraiva Lopes da Silva
Interno: Doutora Ana Maria de Fátima da Silva Martins Gonçalves Reis

2015

Production of lipids (for biodiesel) and carotenoids from the yeast *Rhodotorula glutinis* grown in a bench reactor, in a fed-batch system

João Pedro Rascão Ascensão Caldeira

2015

This thesis was fully performed at Laboratório Nacional de Energia e Geologia (LNEG) under the direct supervision of Maria Teresa Saraiva Lopes da Silva in the scope of the Master in Applied Microbiology of the Faculty of Sciences of the University of Lisbon.

Acknowledgments

I would like to express my sincerest gratitude to Dr. Teresa Lopes da Silva for accepting me into her project, her sympathy, expert guidance, helpful advice and especially for the encouragement and patience during my harshest times for the duration of my research.

Special thanks go to Dr. Sandra Chaves and Dr. Ana Reis for accepting to be my internal supervisors.

I want to thank all my work colleagues. Although my time with you was brief, your collaboration and friendship were very meaningful during my stay and will not be forgotten.

I would like to thank Dr. Carla Santos, Dr. Alberto Reis, Engr. Carlos Barata and Techs. Céu Penedo and Margarida Monteiro for all their help and patience.

My thanks to all my Biochemistry major and Applied Microbiology master's teachers, who provided me with the knowledge required to accomplish my goals.

Many thanks to Drs. Luís Calado and Francisco Pólvora, whose expertise and dedication contributed to my mental wellbeing, allowing me to overcome my insecurities and reminding me to never give up when everything seemed lost.

To my family, particularly my parents for granting me the opportunity to pursue a higher education and for all their support throughout my life.

To my late feline companion. The fond memories of its unconditional love will forever remain in my heart and have helped me smile during my toughest moments.

To my friends for always being there when I need them the most and for all the good times we have shared together.

The present work was carried out within the project FCOMP-01-0124-FEDER-019317 (ex-PTDC/AAC-AMB/116594/2010 entitled ‘‘CAROFUEL - New process for a sustainable microbial biodiesel production: The yeast *Rhodotorula glutinis* biorefinery as a source of biodiesel, biogas and carotenoids’’ supported by FCT (Fundação para a Ciência e a Tecnologia) (also supported by FEDER funding through COMPETE – Programa Operacional Factores de Competitividade).

Resumo

Desde a sua descoberta e exploração que o petróleo se tornou na força motriz da economia mundial e o principal sustento da sociedade moderna, afetando o quotidiano de centenas de milhões de pessoas em todo o Mundo.

Contudo, várias previsões por parte de diversas agências alertam para o esgotamento das suas reservas num futuro próximo pois, uma vez que se tratam de um recurso não-renovável, estas existem em quantidades finitas e não conseguem satisfazer o nível de procura atual porque a sua formação natural à escala humana é tão lenta que as reservas existentes simplesmente são incapazes de aumentar ou ser reabastecidas mais rapidamente do que a taxa a que são extraídas atualmente.

Além da disponibilidade, existe também o problema do impacto ambiental da exploração e combustão de combustíveis fósseis, principalmente as emissões de CO_2 para a atmosfera que estão estreitamente relacionadas com a poluição e as alterações climáticas.

Devido a todos os motivos supramencionados, é urgente encontrar substitutos que satisfaçam as necessidades energéticas mundiais. Entre as diferentes alternativas energéticas existentes, os biocombustíveis representam a opção mais favorável ao meio ambiente.

Os biocombustíveis podem ser classificados como primários ou secundários. Os primários utilizam material orgânico que é queimado diretamente na sua forma química natural e não modificada, utilizado principalmente para o aquecimento e a produção de eletricidade. Os secundários utilizam a biomassa processada que existe na forma sólida, gasosa ou líquida e podem ser usados para o transporte e em vários processos industriais. Os biocombustíveis secundários são ainda classificados como biocombustíveis de primeira, segunda e terceira geração.

Os biocombustíveis de primeira geração são produtos derivados de culturas alimentares para consumo humano. No entanto, a utilização de terras agrícolas aráveis para a sua produção gera alguma polémica, levando a que muitas agências, particularmente organizações agrícolas e alimentares assim como modeladores económicos questionem o uso desses biocombustíveis, considerando-os como inviáveis. De modo a combater esta controvérsia, a produção de biocombustíveis a partir de biomassa não-comestível tem sido favorecida.

Ao contrário dos biocombustíveis de primeira geração, a matéria-prima dos combustíveis de segunda geração provém geralmente de materiais lignocelulósicos não-comestíveis, não competindo com a produção de alimentos, eliminando assim a concorrência com as culturas alimentares. Contudo, estes biocombustíveis não podem ainda ser produzidos economicamente em grande escala, uma vez que a conversão de

biomassa lignocelulósica em açúcares para posterior fermentação é um processo complexo, necessitando de equipamentos de produção e de processamento mais sofisticados, mais investimento por unidade de produção e instalações de grande escala.

Os biocombustíveis de terceira geração utilizam microrganismos como uma alternativa às fontes agrícolas e animais, particularmente microrganismos oleaginosos (aqueles que têm a capacidade de acumular quantidades significativas de triacilgliceróis como materiais de reserva, e apresentam um teor de lípidos superior a 20% do seu peso seco em biomassa) para produção de biodiesel, não apresentando as desvantagens dos biocombustíveis de primeira e de segunda geração.

A maior parte dos trabalhos de produção de biodiesel a partir de microrganismos oleaginosos focam-se na utilização de microalgas autotróficas. Estas crescem mais rápido, apresentam produtividades de biomassa e de lípidos mais elevadas e requerem uma menor área de cultivo comparativamente a culturas vegetais. No entanto, tem-se assistido a uma transição para culturas de microalgas heterotróficas devido a maior facilidade de cultivo e por apresentarem produção mais elevada de ácidos gordos em relação a culturas autotróficas.

Outros microrganismos heterotróficos produtores de óleo, nomeadamente bactérias, fungos e leveduras também têm sido considerados como uma fonte promissora de biocombustível.

A levedura *Rhodotorula glutinis* é uma espécie oleaginosa produtora de carotenóides, produtos de reserva com alto valor acrescentado de grande interesse comercial com aplicações nas indústrias de alimentação animal, farmacêutica e cosmética.

A produção de biocombustíveis de terceira geração é um processo complexo e caro, pelo que, neste aspeto, não traz vantagem em relação aos combustíveis de 1ª geração. Contudo, a coprodução destes compostos intracelulares em conjunto com os lípidos da biomassa da levedura pode contribuir para reduzir significativamente os custos de produção de biodiesel a partir deste microrganismo.

Neste trabalho, a levedura *Rhodosporidium toruloides* NCYC 921 (anamorfo de *Rhodotorula glutinis*) foi cultivada num bioreactor de 7 L com um volume de trabalho de 5 L num sistema semi-contínuo com o objetivo de se otimizar a produção de ácidos gordos (para a produção de biodiesel) e de carotenóides.

A estratégia geral de cultivo consistiu em dois passos distintos. Numa primeira fase, após o desenvolvimento da cultura de levedura em regime descontínuo, uma solução de nutrientes foi fornecida de modo a prolongar a fase de crescimento da levedura. Na segunda fase, assim que a levedura atingiu a fase estacionária, a solução de alimentação foi substituída por uma solução de glucose concentrada (600 $g.L^{-1}$) para

induzir a síntese de materiais de reserva intracelulares, tais como lípidos e carotenóides.

Foram realizados quatro ensaios no total. Cada ensaio durou, em média, uma semana, tendo sido recolhidas, pelo menos, três amostras por dia. Para cada amostra, foram analisados vários parâmetros incluindo a estimativa da concentração de glucose residual por meio de um teste qualitativo utilizando tiras de medição da concentração de glucose, valor de pH e a leitura da absorvência a um comprimento de onda de 600 nm. Outros métodos analíticos incluíram a determinação da concentração de azoto e glucose residuais, teor de lípidos totais e teor e composição em ácidos gordos.

A primeira e últimas amostras recolhidas a cada dia também foram analisadas por citometria de fluxo, com o objetivo de detetar, em tempo real, o teor de carotenoides totais, assim como a viabilidade celular analisando a integridade da membrana citoplasmática e o potencial da membrana mitocondrial em simultâneo por medição da fluorescência emitida por células de levedura duplamente coradas com os fluorocromos iodeto de propídio e 3,3'-dihexiloxacarbocianina [DiOC6 (3)], respectivamente.

Os dois primeiros ensaios foram realizados a valores de pH constantes. O primeiro foi realizado a pH 5,5, enquanto o pH no segundo ensaio foi alterado para 4,0 com o objetivo de melhorar a produtividade de biomassa e a produtividade em ácidos gordos.

A alteração de pH no ensaio II resultou num aumento de 23,08% na concentração máxima de biomassa (119,61 $g.L^{-1}$) e um aumento de 10,23% da produtividade máxima de biomassa (1,76 $g.L^{-1}$) em comparação com o ensaio I. No entanto, o teor em ácidos gordos, percentagem total de lipídios e concentração de carotenóides no ensaio II foram menores do que no ensaio I devido a problemas associados à limitação de oxigénio.

Para os ensaios III e IV, o pH do meio de cultura foi ajustado a 4,0 durante a fase de crescimento da levedura e, uma vez que a cultura atingiu a fase estacionária, foi novamente ajustado para a 5,0 para promover a acumulação de produtos lipídicos de armazenamento, tais como os carotenóides. A única diference entre os ensaios III e IV foi a utilização de uma turbina adicional adaptada ao eixo do rotor do bioreactor para o ensaio IV, de modo a garantir uma transferência de oxigénio mais eficiente no meio de cultura. O ensaio IV foi o que apresentou os resultados mais satisfatórios, obtendo-se valores mais elevados da concentração de biomassa (154,21 $g.L^{-1}$), produtividade de biomassa (2,35 $g.L^{-1}.h^{-1}$), produtividade de ácidos gordos (0,40 $g.L^{-1}.h^{-1}$), produtividade de carotenóides (0,29 $g.L^{-1}.h^{-1}$) teor total de carotenóides (0,29 $mg.g^{-1}$) e percentagem de lípidos totais (41,07%) face aos restantes ensaios.

Palavras-chave: biocombustíveis, biodiesel, *Rhodotorula glutinis*, *Rhodosporidium toruloides*, carotenoides, ácidos gordos, semi-contínuo, citometria de fluxo

Abstract

In this work the yeast *Rhodosporidium toruloides* NCYC 921 was grown in a 7 L bioreactor with a 5 L working volume in a fed-batch system with the aim of optimizing production of fatty acids (for biodiesel purposes) and carotenoids, a high-value added product with commercial interest. Several different cultivation strategies were studied.

The first two experiments were performed at constant medium pH. The first fed-batch was carried out at a medium pH of 5.5, while the pH in the second assay was changed to 4.0, with the goal of enhancing biomass productivity and to further improve fatty acid and carotenoids productivities.

A dual-stage strategy was used in the third fed-batch cultivation, with the yeast growth phase conducted at pH 4.0 and the stationary phase, where products accumulation occurs, was conducted at pH 5.0. These conditions were kept for the fourth assay, with the exception of an additional impeller adapted to the bioreactor's rotor shaft in order to improve the oxygen transference in the broth.

Assay four achieved the highest biomass concentration (154.21 $g.L^{-1}$), biomass productivity (2.35 $g.L^{-1}.h^{-1}$), fatty acid productivity (0.40 $g.L^{-1}.h^{-1}$), total carotenoid concentration (0.29 $mg.g^{-1}$), carotenoid productivity (0.29 $mg.L^{-1}.h^{-1}$) and total lipid content (41.07%), showing that the dual-stage strategy was successful and also that oxygen plays an essential role during the yeast cultivation, particularly in the carotenoid synthesis.

Flow cytometry was used to monitor, in real time, total carotenoid content and cell viability (membrane potential and membrane integrity) throughout the yeast cultivations. The data obtained revealed a correlation between carbon source starvation, oxygen deficiency and damaged yeast's cells.

Keywords: *Rhodosporidium toruloides*, biodiesel, fatty acids, carotenoids, fed-batch, flow cytometry.

Index

Figure index

Table index

Equation index

List of abbreviations and symbols

$(NH_4)_2SO_4$ - Ammonium sulphate

$AlCl_3.6H_2O$ - Aluminum chloride hexahydrate

ASPO - Association for the Study of Peak Oil and gas

B – Batch cultivation

$C_{15}H_{15}N_3O_2$ – Methyl red

$C_{16}H_{18}N_3SCl$ – Methylene blue

$C_{18}H_{36}O_2$ – Stearic acid

$CaCl_2.2H_2O$ - Calcium chloride dihydrate

CO_2 – Carbon dioxide

$CoCl_2$ - Cobalt chloride

$CuCl_2.2H_2O$ - Copper chloride dihydrate

$CuSO_4$ – Copper sulfate

DCW – Dry cell weight

DiOC6 (3) - 3,3-dihexyloxacarbocyanine iodide

DMSO – Dimethyl sulfoxide

DNS - 3,5-dinitrosalicylic acid

DO – Dissolved oxygen percentage

EN – European norm

FA – Fatty acids

FAME – Fatty acid methyl ester

FB – Fed-batch cultivation

FC – Flow cytometry

$FeSO_4.7H_2O$ - Ferrous sulphate heptahydrate

FID – Flame ionization detector

FL – Fluorescence detector

G – Concentrated glucose solution

GC – Gas chromatography

H_2SO_4 – Sulfuric acid

H_3BO_3 – Boric Acid

HCl – Hydrochloric acid

HPLC – High performance liquid chromatography

IEA – International Energy Agency

IPCC – Intergovernmental Panel on Climate Change

K_2SO_4 – Potassium sulfate

KH_2PO_4 - Potassium dihydrogen phosphate

k_La - Volumetric oxygen transfer coefficient

$KNaC_4H_4O_6 \cdot 4H_2O$ – Potassium sodium tartarate

MEA – Malt extract agar

$MgSO_4.7H_2O$ - Magnesium sulphate heptahydrate

$MnSO_4.7H_2O$ - Manganese sulphate heptahydrate

MUFA – Monounsaturated fatty acids

Na_2HSO_4 - Sodium sulphate anydrous

$Na_2MoO_4.2H_2O$ - Sodium molybdate dihydrate

NaOH – Sodium hydroxide

NG – Nutrients with glucose solution

OD – Optical density

PBS – Phosphate buffer saline

PI - Propidium iodide

PO – Peak oil

PPG – Polypropylene glycol

PUFA – Polyunsaturated fatty acids

SFA – Saturated fatty acids

TAG - Triacylglycerol

TC – Total carotenoids

TEA – Triethylamine

TiO_2 – Titanium dioxide

$ZnSO_4.7H_2O$ - Zinc sulphate heptahydrate

1. Introduction

1.1. Fossil fuel: The issue of peak oil and the need for biofuels

The exploration and use of fossil fuels by mankind is an ongoing practice that has persisted for millennia and increased significantly about 250 years ago during the dawn of the Industrial Revolution, becoming the center of growth and trade [**1-3**]. Several major changes in our civilization since the beginning of the 20th century have increased dependence on a convenient energy source, mainly crude oil [**1**].

Fossil energy has grown from insignificant levels in 1800 to an annual output of nearly 10.000 million tons of oil equivalents [**3**] and still remains the driving force of current world economy and backbone of modern society, affecting the everyday lives of hundreds of millions of people worldwide to a point where it is considered an addiction [**1**]. Nowadays, fossil fuel accounts for 86% of global primary energy demand, with crude oil as the greater component, accounting for 36% demand followed by coal and natural gas at 27% and 23% respectively [**4, 5**], of which 58% alone is consumed by the transport sector [**6**].

Recent forecasts by the International Energy Agency (IEA) [**7**], BP [**8**] and Intergovernmental Panel on Climate Change (IPCC) [**9**] indicate a future increase of fossil fuel demand. However, all fossil fuels are non-renewable energy sources thus they obviously exist in finite quantities and cannot continue to meet this rising demand because their natural formation on a human scale is so slow (requires millions of years to create) that it simply cannot augment or replenish them faster than the rate at which they are currently being extracted [**1- 3, 10, 11**].

Concerns about natural resources depletion is not a recent issue, having been discussed since the end of the 18th to mid 19th centuries [**12, 13, 14**]. However, an accurate model for predicting production of finite resources was first published in 1956 by geophysicist M.K. Hubbert (1903-1989) [**15**] who, despite great controversy at that time [**1**], correctly predicted that the peak oil (PO) in the US lower 48 states would occur in 1970 [**1-3, 5**]. His theory, now named the “Hubbert Peak Theory”, represents the production tendency of non-renewable resources by a symmetric bell-shaped curve [**1, 2, 5, 11, 16**] where production initially increases and eventually reaches its maximum, represented by a peak or a plateau, after which inevitably starts to decline [**4, 11, 16, 17**]**.** This happens because, initially, the extraction of an abundant and cheap resource leads to economic growth and investments increase, promoting further extraction [**16**]. Then, resources gradually become technically, energetically and economically more difficult to extract [**4**] (e.g. due to a fall in oil rig pressure and/or water infiltration [**17**]) and in time, lack of investment and rising prices result in slowed growth and, eventually, production starts falling to zero [**16**].

The concept of PO is now well accepted and Hubbert's theory continues to be the most widespread production prediction method used for fossil fuels [**1**].

When the global production peak will exactly happen is still unknown. In 1998 two geologists, Jean Laherrère (1931-) and Colin J. Campbell (1931-), based on Hubbert's research, published their own prediction of PO [**18**] which was expected to happen before 2010. Its influence led to the foundation of the Association for the Study of Peak Oil and gas (ASPO), the first and still the most important international organization which focuses on the study of PO [**1**].

The ASPO offers a pessimistic view of PO from a geological standpoint [**3, 10**], supporting that oil deposits are fixed and, as a consequence, stocks decrease with consumption. It also expresses concern over decreasing production, stating that all the largest, therefore easier to locate, reserves have already been explored and future discoveries will be made in smaller and more remote areas and criticizes overestimation made by producing countries whose political and economic objectives may encourage reserve misreporting for their own benefit [**2**, **10**]. According to these statements, the effective PO date should not be very distant [**1**].

The opposing, optimistic side is represented by economists [**3, 10**] who disagree with the geologists' overly pessimistic opinions. Although they don't dismiss the possibility of PO from ever happening, their main argument is that there is no reason to worry because available resources are big enough and that it will only occur after several decades [**16**].

It is this lack of consensus that increases speculation as to when PO will actually take place, with time periods ranging from 2010 to 2040 [**10**]. Whichever the calculated date, signs of crude oil exhaustion are becoming more evident [**1**] and sooner or later it will completely run out.

Besides availability, there is also the problem of environmental impact from exploring and combusting fossil fuels, mainly CO_2 emissions into the atmosphere, which are closely related to pollution and climate change, with levels expected to rise in the future [**2-5, 6-11, 19-22**]. Peaking of conventional (fossil) oil also plays a role in the environment because scarcity of conventional reserves, which are the most accessible and whose production poses less technical challenges [**2**], will result in production switching to dirtier unconventional oils (e.g. tar sands) [**16**] that have larger emission footprints [**2, 3**] due to their extraction being capital intensive and requiring additional energy [**2**].

Due to all the aforementioned reasons, attention has shifted towards development of renewable, biodegradable, cheap, sustainable, environmental friendly, freely available in nature and efficient alternative energies [**6, 19, 20**].

Among several fossil fuel substitutes, biofuels, hydrogen, natural gas and synthesis gas are seen as the most sustainable [**6**]. Within these four, biofuels are the most environment-friendly choice; hence, biofuels are now being explored [**6**].

Biofuels are referred to liquid, gas and solid fuels predominantly generated from biological material [**6, 20, 22**]. The available types of biofuels are bioethanol, renewable methanol, biodiesel, biogas, biobutanol and biohydrogen [**20**] and are the answer to reducing both dependence on fossil energy and greenhouse gases (GHG) emissions as well as providing steady income for farmers [**6, 23**].

1.2. First, second and third generation biofuels

Classification of biofuels falls under two categories: primary and secondary. The first category is defined by organic material that is directly combusted in its natural and non-modified chemical form (e.g. fuelwood, wood chips and pellets, etc.), used primarily for heating, cooking and producing electricity. The second comes from processed biomass that exists in solid, gas or liquid forms and can be used for transportation and in various industrial processes [**6, 23**]. Secondary biofuels are further categorized in to first, second and third-generation biofuels [**6, 23**].

First and second generation biofuels share the same biotechnological background: conversion of carbohydrates to alcohol and/or methane gas and biodiesel production through fatty acid hydrolysis with methanol in the presence of a catalyst to glycerol and long chain alkyl esters (diesel) in a transesterification reaction [**24**]. The difference between the two is the feedstock [**24**].

First-generation biofuels are derived from food crops for human consumption (rice, wheat, barley, potato wastes, sugar beets etc.) and vegetable oils (soybean oil, sunflower oil, corn oil, olive oil, palm oil, coconut oil, rapeseed oil, mustard oil, castor oil etc.) [**19, 22, 24, 25**]. The most well-known first-generation biofuel is bioethanol [**6**] using sugar-cane as a common feedstock, Brazil being the main country that produces and uses it [**19, 22**]. Nonetheless, first-generation biofuels raise some concerns regarding its sustainability. With global population steadily increasing, more food will be required to meet its needs. As the production capacity of first-generation biofuels increases, so does their conflict with food supply due to pressure on agricultural land (e.g. the intensive use of land with high fertilizer and pesticide applications and water) leading to environmental problems, rise in costs and hunger threats from food shortages, especially in developing countries where more than 800 million people suffer from hunger and malnutrition [**6, 23, 25-29**]. Consequently, many agencies, particularly food and agricultural organizations and economic modelers consider the use of these biofuels as unviable [**28**] and efforts are being made to use non-edible biomass for the production of biofuels [**6**].

Second-generation biofuels emerge as a solution to the food versus fuel controversy because, unlike first-generation biofuels, they do not compete with food production as their feedstock generally comes from non-edible lignocellulosic rich materials, eliminating competition with food crops [**6, 22-24, 27**]. Examples of different feedstocks include *Jatropha curcas*, lesquerella oil, cotton seed, *Pongamia glabra*, karanja and *Salvadora oleoides*, linseed oil, forestry residues, switch grass, wood and biomass sources [**20**]. Second-generation biofuels offer a number of advantages. Some feedstock species can be grown in largely unproductive areas and are mostly located in degraded forest and coastal areas; they are biodegradable and are 15–20% more efficient when mixed with petroleum diesel in different proportions without the need to modify engines and emit less carbon gases [**20**]. They also exhibit desirable fuel properties such as high cetane number, very high flash point, excellent lubricity and very favorable energy balance [**20**]. However, second-generation biofuels cannot yet be produced economically in a large scale, since converting the lignocellulosic biomass into fermentable sugars is a complex process [**22-24**]. Therefore, production of second-generation biofuels requires more sophisticated processing equipment, more investment per unit of production and large-scale facilities [**6**].

Third generation biofuels focus on microorganisms [**6**] as an alternative to agricultural and animal sources [**30**], particularly oil-accumulating microbes such as microalgae, bacteria, yeasts and other fungi [**31**] whose oil can be extracted and converted into biodiesel. Biofuels from microorganisms are devoid of the major disadvantages related with biofuels derived from plant crops [**6**] since their cultivation isn't dependant on seasons and climate, presenting properties similar to vegetable oil [**32**].

A microorganism is considered to be oleaginous if it has the capability to accumulate significant quantities of storage triacylglycerols (TAGs) [**33**] and a lipid content exceeding 20% of their dry biomass weight [**30, 34-36**]. Lipid accumulation in these microorganisms is dependent on nitrogen availability [**30**]. Once this nutrient is exhausted, the excess carbon present is assimilated by the cells and converted into TAGs during the stationary phase, when cell growth and division is halted, and lipid accumulates within existing cells [**30**].

Third-generation biofuels production mainly focuses on microalgae [**23**]. Microalgae, as a feedstock for third-generation biofuels production, are inexpensive, environmentally friendly, fully renewable, and can be used in a wide range of fuel blends such as diesel, petrol, and jet fuel and aviation gasoline [**20**]. Generally they have higher biomass and lipid productivities and grow faster when compared to oilseed crops [**26**]. Species such as *Chlorella* contain around 60-70% lipid content and high lipid productivity (7.4 $g.L^{-1}.d^{-1}$ for *Chlorella protothecoides*) [**22**], need much less land area (up to 49 or 132 times less)

and can have up to 100 times more oil content when compared to oilseed crops [**26, 28**], reaching 5000 gallons per acre, in contrast with 1000 gallons per acre from common vegetable oils. They are able to produce, theoretically, up to a yield of 20,000 gallons of feedstock per acre of land, depending on the species [**28**]. The estimated market size for algae is $425 billions, which is more than twice the expected market size for other traditional biofuels [**28**].

Microalgae can be either autotrophic or heterotrophic [**23**]. Autotrophism uses inorganic carbon sources, and can be further classified according to the source of energy either in to photoautrophism (autotrophic photosynthesis) if using light or chemoautotrophism if the energy comes from oxidized inorganic compounds. Heterotrophic microalgae require an organic carbon source to grow. Like in autotrophism, they can be categorized according to the energy source in to photoheterotrophs or chemoheterotrophs. Some strains can combine autotrophic photosynthesis and heterotrophic assimilation of organic compounds, called mixotrophs. [**6, 23, 29, 37**]

At present, most of the works aiming at microbial biodiesel production use autotrophic microalgae [**29, 38**] to limit cost of input materials [**31**]. Indeed they are efficient CO_2 fixers, requiring considerable amounts of this greenhouse effect gas to convert it into biomass using solar energy, they can be used as a cheaper mode of CO_2 sequestration in oil and gas facilities and related industrial power plants, and are considered almost carbon neutral [**26, 28**]. However, their growth is much slower than bacteria or fungi. Moreover, autotrophic cultures have low biomass and oil yields, due to limitations of light and oxygen accumulation [**38**], are dependent on climate, are easily contaminated by other microorganisms and require large areas and high amounts of water [**31**]. Thus, future research should be focused on heterotrophic cultivation [**29**].

Heterotrophic algae cultivation systems are carried out in the absence of light. Therefore, it is easy to cultivate them at large scales without depending on light requirements [**29**]. Despite the additional cost from having to provide the culture with the carbon source, heterotrophic systems easily compensate for this due to increased oil content and cell density in a shorter time [**31**]. A specific study by Liu *et al* [**39**] shows the benefits of using heterotrophic algae for biodiesel production, with a 900% increase in lipid yield using the heterotrophic *Chlorella zofingiensis* compared to autotrophic conditions.

In addition to heterotrophic microalgae, other heterotrophic oleaginous microorganisms such as bacteria, filamentous fungi and yeasts have been considered as potential source oil for biodiesel production, because they can produce appreciable amounts of lipids when cultured in conventional bioreactors and under strictly controlled conditions (which reduces the risk of contaminations), reaching higher biomass and lipid yields [**40**].

Although bacteria have higher growth rates and shorter growth periods than microalgae, most of the species have lower lipid content, on average 20-40% of dry biomass [**30**]. However, only a few strains are known to synthesize lipids and, since they are stored in the outer membrane, it is difficult to extract them efficiently [**30**]. For these reasons, there is currently no industrial application of bacterial feedstocks for biofuel production [**30**].

For decades, oleaginous yeasts have been studied as a microbial source of oil [**31**]. Compared to microalgae, conventional microbial bioreactors can be used to cultivate these microorganisms, resulting in improved biomass yield and, consequently, lesser biomass and oil production costs [**35**].

Of 600 known yeast species [**41**], over 70 are considered oleaginous and oleaginicity screenings are still uncovering new oil producing yeast species [**31**]. These species are generally from, but not limited to, the genera *Candida*, *Cryptococcus*, *Rhodotorula*, *Rhizopus*, *Trichosporon*, *Lipomyces*, and *Yarrowia* and can accumulate lipids 40-70% of their biomass depending on the conditions in which they are grown [**41**].

1.3. The yeast *Rhodosporidium toruloides*

Species of the genus *Rhodotorula* date all the way back to Fresenius in 1850 with the description of *Cryptococcus glutinis* [**42**]. The genus was formally described by Harrison in 1928 [**43**] to include red yeasts that did not produce spores while other pigmented yeasts were placed in *Chromotorula*, a genus that would be later rejected by Lodder in 1934 [**44**] who attributed the genus *Rhodotorula* to all carotenoid producing species.

In the first edition of the book entitled “The Yeasts, A Taxonomic Study”, *Rhodotorula* yeasts were notable for seldom exhibiting primitive pseudomycelia, synthesizing carotenoids and lacking fermentation [**45**]. Seven species were accepted in this edition. Supplementary descriptions were made in the second edition published in 1970, adding *Rhodotorula*’s inability to assimilate inositol and to synthesize starch-like compounds [**46**]. Nine species were recorded in the genus.

By this time, studies on the sexuality of *Rhodotorula* confirmed its basidiomycetous nature. Investigations by Banno, I. led to the observation that, in *Rhodotorula*, conjugation of haploid cells gave rise to a mycelial stage presenting a dikaryotic mycelium with clamp-connections, indicating a correspondence to a secondary mycelium of Basidiomycetes, concluding that the *Rhodotorula* yeasts capable of mating are simply the haploid stage of a basidiomycetous fungus [**47, 48**]. The perfect name given to the two sexually compatible strains of *Rhodotorula glutinis* which Banno studied is Rhodosporidium toruloides Banno, the type species of the genus [**49**].

This major finding changed the definition of the genus *Candida*. Ascomycetous species were retained in this genus while the basidiomycetous species were separated based on

the composition of cell hydrolyzates [**50**]. Species with xylose in the cell hydrolyzates were placed in *Cryptococcus* and those which lacked xylose were transferred to *Rhodotorula* [**50**].

The *Rhodotorula* genus, as currently defined, includes 34 species that comprise a polyphyletic group of organisms. Cultures have a coral pink color, are smooth and moist to mucoid, with variable growth at 37ºC with a diameter between three to five micrometers and grow as ellipsoid, multipolar budding yeast [**51**].

Rhodotorula glutinis is one of the 34 species, classified taxonomically in the super-kingdom *Eukaria*, kingdom *Fungi*, sub-kingdom *Dikaria*, phylum *Basidiomycota*, sub-phylum *Puciniomycotina*, class *Microbotriomycetes*, order *Sporidiobolales* and genus *Rhodotorula* [**52**]. No family has yet been assigned [**53**].

Compared to algae, fungi and bacteria, *Rhodotorula glutinis* exhibits higher growth rate and can accumulate lipids under low-cost substrates [**32**].

Rhodosporidium toruloides NCYC 921 is an anamorph of this yeast [**54, 55**].

1.4. Carotenoids

Carotenoids are isoprenoids containing a characteristic polyene chain of conjugated double bonds and are either acyclic or cyclic with one or two cyclic end groups [**56**]. There is a great variety of carotenoids, with more than 600 different compounds [**56-60**].

Carotenoids are important in nature as they confer color to plants and animals specifically birds, insects, fish, and crustaceans [**57**]. The coloration of flamingoes and salmon is a common example of pigmentation from the presence of the carotenoid astaxanthin [**59**]. Other carotenoids can also give purple, crimson and burgundy colors to feathers of some birds [**59**].

Carotenoid synthesis is present in plants, bacteria, fungi, and algae [**57**]. Animals lack this ability, and are therefore only able to incorporate them from their diet [**57**]. Of all the existing carotenoids, about 40 are found in the human diet and less than half of these are known to be present in humans [**61**], with 90% of the carotenoids in the diet and human body represented by α-carotene, β-carotene, lycopene, lutein and cryptoxanthin [**58**, **60**].

Intake comes primarily from fruits and vegetables [**62**]. Yellow and orange fruits and vegetables and green leafy vegetables contain β-carotene whilst α-carotene is mainly found in carrots. Tomatoes and tomato based foods account for over 85% of all dietary sources of lycopene; spinach and kale are a source of high levels of lutein and zeaxanthin; orange fruits, such as tangerine and papaya, have large amounts of β-cryptoxanthin [**58, 62**]. Additionally, smaller carotenoid amounts can be obtained from

dairy products, egg yolks, and ocean fish and in colorants added to processed foods [**58**].

Increasing commercial interest of carotenoids is connected to their potential benefits in human and animal health [**63**]**.** Carotenoids are seen as biomarkers, as they have the potential to give an accurate estimate of a person's overall health [**59**]. Many clinical trials show a positive association between dietary carotenoids and decreased risk of several disorders such as cardiovascular disease, cancer, age-related progressive eye loss and cognitive decline [**57-65**] due to their physiological functions such serving as vitamin A precursors and antioxidants [**57-66**].

Carotenoids are currently used in feed, pharmaceutical and cosmetics industries and have high commercial value with a global market accounted for 766 million dollars expected to increase by 155 million dollars in the current year [**67**]

Despite the availability of a variety of natural and synthetic carotenoids, microbial sources of carotenoids have received increasing attention because of the restricted rules and regulations currently applied to chemically synthesized/purified pigments [**65**]. Among these sources, *Rhodotorula* sp. is a well known carotenoid producer [**63, 65**]. The 4 main carotenoids produced by this species are torularhodin, torulene, γ-carotene and β-carotene [**68**] (Figure 1).

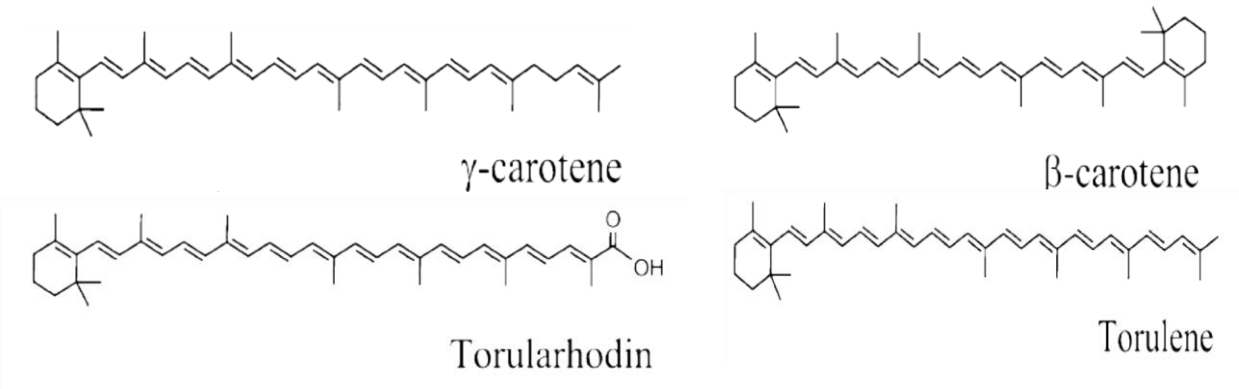

Figure 1. Chemical structure of **γ**-carotene, β-carotene, torularhodin and torulene, the 4 main carotenoids produced by *Rhodotorula* sp. (Adapted from Moliné *et al.* [**68**]).

Yeasts are better suited than algae or molds for large-scale carotenoid production in fermenters, due to their unicellular nature and high growth rate [**63**]. Besides, yeasts can adapt to different environmental conditions and grow under a wide variety of carbon and nitrogen sources [**68**].

1.5. Sustainable production of biodiesel from *Rhodosporidium toruloides*

Currently, the production of biodiesel from microorganisms is not economically feasible because it is an expensive process compared to first generation fuels [**54**].

However, *Rhodosporidium toruloides* biomass has a high lipid content and is also rich in high-value added products such as carotenoids (section 1.4.). The co-extraction and commercialization of these two products may help reduce the overall process cost [**54**, **55**].

2. Scope of present study

This work's main objective was to optimize production of lipids and carotenoids by the oleaginous yeast *Rhodosporidium toruloides* NCYC 921 using a bench bioreactor operating in a fed-batch regime, with glucose as the carbon source. Different medium pH changes strategies were used in order to improve lipids and carotenoids production.

Flow cytometry (FC) was used to monitor, in real time, various cell parameters such as total carotenoids (TC) content and cell viability.

On a personal level, this work was conducted as part of a master's thesis in order to assimilate the maximum of experimental techniques and as much knowledge possible.

3. Materials and methods

3.1. Reagents and equipment

The list of all reagents used throughout the whole experimental work can be found in table A1 (see annex I.). All equipment will be mentioned along this section.

3.2. Microorganism

The strain used was *Rhodosporium toruloides* NCYC 921, supplied by the National Collection of Yeast Cultures (Norwich, United Kingdom).

Yeast cells were kept in Malt Extract Agar (MEA) (in $g.L^{-1}$: agar, 15; malt extract, 30; mycological peptone, 5) slants at 4ºC until needed.

3.3. Pre-inoculum preparation

Pre-cultures were prepared by transferring *R.toruloides* cells from two MEA slants at 30ºC for 72 h to 1 L baffled flasks containing 150 mL of sterilized growth medium. The glucose solution (35 $g.L^{-1}$) was sterilized separately and mixed aseptically.

Medium pH was adjusted to 4 before transferring the yeast cells. Shaken incubation was performed at 30ºC at 150 rpm (Unitrom Infors, Switzerland) for 24 hours (exponential growth phase).

All pre-cultures were performed in duplicate to account for any possible contamination.

3.4. Bioreactor growth medium

The growth medium described by Pan et al (1986) was used [**69**]. Compositions are as follows:

Table 1. Composition of the growth medium (values in $g.L^{-1}$)

Culture medium	$g \cdot L^{-1}$
KH_2PO_4	12.5
Na_2HSO_4	1.0
$(NH_4)_2SO_4$	5.0
$MgSO_4.7H_2O$	2.5
$CaCl_2.2H_2O$	0.25
Yeast Extract (YE)	1.9
Glucose	35
Trace Minerals	-

Table 2. Composition of trace minerals used in the growth medium (values in $g.L^{-1}$)

Trace Minerals ($0.25\ mL.L^{-1}$)	$g \cdot L^{-1}$ (in 5N-HCL)
$FeSO_4.7H_2O$	40
$CaCl_2.2H_2O$	40
$MnSO_4.7H_2O$	10
$AlCl_3.6H_20$	10
$CoCl_2$	4
$ZnSO_4.7H_2O$	2
$Na_2MoO_4.2H_2O$	2
$CuCl_2.2H_2O$	1
H_3BO_4	0.5

3.5. Fermentation in a bioreactor

Fed-batch microbial cultivation trials were carried out in a fermenter (Electrolab Fermac 310/60 bioreactor, United Kingdom) with a 5 L working volume (total volume 7 L). The vessel initially contained 2.85 L of concentrated cultivation media with a salt concentration for 5 L, and 35 $g.L^{-1}$ glucose with 1.25 mL trace minerals.

Temperature control was achieved using a PT100 sensor to measure vessel temperature and a low voltage (24 V) control wrap-around heating system with a cold finger heat exchange for cooling.

The pH was monitored by an autoclavable pH electrode and adjusted by automatic addition of 5 M HCl or 5 M NaOH using two separate peristaltic pumps (Watson Marlow).

Dissolved oxygen (DO) was monitored by an autoclavable polarographic DO electrode, controlled by stirrer speed, air flow, or combination of both.

Polypropylene glycol (PPG) was used as an anti-foaming agent, added by an automatic peristaltic pump, controlled by a conductivity probe.

The feeding strategy consisted of two distinct steps. In an initial phase, after a previous batch culture, a nutrient solution (in $g.L^{-1}$: $MgSO_4.7H_2O$, 9; Yeast Extract, 20; Glucose, 600) was supplied to the yeast to extend its exponential phase. Secondly, once the yeast reached the stationary phase, the feeding solution was replaced by 600 $g.L^{-1}$ concentrated glucose solution to induce the synthesis of intracellular storage materials such as lipids and carotenoids.

Fermentations lasted a week on average, and three samples were collected per day. For each sample, several parameters were analyzed including the estimation of the residual glucose concentration, by means of a qualitative test using Combur-Test® strips, pH value (Consor C3021, Belgium) and absorbency at 600 nm (ThermoSpectronic Genesys 20). The first and last samples collected per day were also analysed by flow cytometry to evaluate at-line cell viability (section 3.8.1) and carotenoid content (section 3.8.2).

The contents of the three samples were then centrifuged for 10 min at 9000 rpm at 5ºC (Avanti J-25 I Centrifuge Beckman, USA) and the supernatant stored at -18 ° C for further analysis of residual glucose (section 3.6.2) and nitrogen (section 3.6.3). The biomass (pellet) was also stored at -18 ° C for further analysis of fatty acids (section 3.6.4) and total lipids (section 3.6.5).

3.6. Analytical Methods

3.6.1. Biomass quantification

Biomass was measured by optical density (OD) at 600 nm wavelength in a spectrophotometer (ThermoSpectronic® Genesys 20, Portugal).

A linear regression was used to establish the correlation between OD and dry cell weight (DCW). This correlation is expressed by the equation: $OD_{600\ nm} = 0.7062\ [biomass] + 0.4338$ ($R^2 = 0.9986$).

3.6.2. Residual glucose concentration

Residual reducing sugar concentration was determined by the 3,5-dinitrosalicylic acid (DNS) method [**70**].

From a glucose stock solution (1.5 $g.L^{-1}$), six standard solutions were made by performing serial dilutions, in distilled water, with concentrations ranging from 1.5 g/L to 0.75 g/L with a 10 mL final volume (10, 8, 5, 1, 0.5, 0) in order to establish a calibration curve to determine the glucose concentration in the samples. Supernatant samples were diluted appropriately so that absorvance values would not deviate from those registered in the calibration curve.

To a 0.5 mL sample volume, 0.5 mL DNS reagent [5g DNS, 8g NaOH and 150g potassium sodium tartarate ($KNaC_4H_4O_6 \cdot 4H_2O$), in 500 mL distilled water] was added. The

mixture was vortexed fo 5 seconds, sealed and placed in a boiling water bath for 5 min, followed by 5 min in an ice bath to stop the reaction. The mixture was diluted in distilled water (5 mL) and vortexed once more. Sugar concentration was determined according to samples' spectrophotometrical readings at a 550 nm wavelength. Standard solutions and samples were analysed in duplicate and triplicate, respectively.

3.6.3. Nitrogen quantification

Quantification of total nitrogen was done according to the classical Kjeldahl method [**71**]. Supernatant samples (5 mL) were weighed in Kjeldahl digestion tubes with a 800 mL capacity. Conversion of amino nitrogen of organic components present in the samples into ammonium sulphate occured for 2 to 3 hours in the presence of 12 M H_2SO_4 and a catalyst [30g copper sulfate ($CuSO_4$), 30g titanium dioxide (TiO_2), 10g stearic acid ($C_{18}H_{36}O_2$) and 930 g potassium sulfate (K_2SO_4)] until samples became pale green, indicating complete digestion.

Ammonia was distilled from an alkaline solution (NaOH 50%) and absorbed in a 4% H_3BO_3 solution containing two drops of pH indicator (2g methyl red and 1g methylene blue in 100 mL 95% (v/v) ethanol).

Ammonia content was determined by titration with 0.1 N HCl, with the indicator's colour shifting from green to violet once the pH reached 4.8. Total nitrogen percentage in each sample is given by the following equation:

$$N = \frac{0.14\mathrm{V}}{m}$$

Equation 1 - Nitrogen content, given in percentage (nitrogen mass / 100 mL sample). V = Volume in mL 0.1 N HCl used in sample titration. m = sample mass expressed in grams.

3.6.4. Derivatization and identification of fatty acids

Fatty acid methyl esters (FAME) were obtained according to the method described by Lepage and Roy (1986) [**72**], modified by Cohen *et al* (1988) [**73**].

Transesterification was accomplished by adding 2 mL methanol/acetyl chloride (95:5, v/v) and 0.2 mL internal standard [heptadecanoic acid, 17:0 (5 $mg.mL^{-1}$, Nu-Check-Prep, Elysian, USA) to 0.1 g freeze-dryed (Heto® PowerDry LL3000 Freeze Dryer with Vacuubrand® vacuum pump) yeast biomass. The mixture was sealed under a saturated nitrogen atmosphere and heated at 80ºC for 1 h, protected from light.

After cooling to room temperature, samples were diluted with 1 mL water to facilitate phase formation. Extraction was made with 1 mL n-heptane. The heptanoic (upper) phase was filtered through a cotton and anydrous sodium sulphate filter and collected into light-protected teflon-lined vials under nitrogen atmosphere. Analysis was performed

in a gas chromatograph (SCION GC 436 with Kombi Moisture/HydroCarbon Filter helium, air and hydrogen filters also from Bruker, Germany) equipped with a flame ionization detector (FID). Separation of the compounds was carried out on a 30 m long Supelcowax 10 (Supelco) capillary column with a 0.32 mm internal diameter and 0.25 mm film thickness. The initial column temperature was programmed to 200ºC for 20 min until it reached a final temperature of 220ºC. Injector and detector temperatures were 250ºC and 280ºC, respectively. Helium gas was used as carrier at a flow rate of 1.3 ml/mL. Methyl esters were identified by comparison of retention times of the standard components 461 (Nu-Chek-Prep, Elysian, MN, USA).

Extractions were performed in duplicate and injected twice. Quantification of individual fatty acids was done in accordance with the following equation:

$$mFA = \frac{AFA}{AIS} \times RFFA$$

Equation 2 - Quantification of fatty acids. mFA = amount of fatty acid; AFA = fatty acid peak area; AIS = area of the peak corresponding to the internal standard (17:0); RFFA = fatty acid response factor (RF = 1 for all fatty acids).

3.6.5. Total lipids extraction

The protocol chosen for evaluation of total yeast lipid content was adapted from a standard method for determination of oil content in oleaginous seeds [**74**].

Freeze-dryed *R. toruloides* cells were broken in a ball mill (Retsch® MM 400 ball mill) set to its maximum vibrational frequency for 3.5 min using 10 cm diameter metal spheres. This process was facilitated by previously grinding and crushing the dry biomass using a mortar and pestle.

One gram of ruptured cells was weighed into a porous cellulose thimble, which was then tightly packed and loaded into a Soxhlet apparatus. Continuous extraction lasted for a total of 9 hours, with hexane (100 mL) as the organic solvent.

The solvent containing the oils (noticeable by its bright orange colour) was collected into tared (sonicated for 15 min in regular tap water, then thoroughly washed with deionized water, ethanol and acetone prior to being placed in an oven at 100ºC for 16 hours) round base flasks. The deoiled biomass left inside the thimble was stored at -20ºC. Oil extracts that were cloudy, due to some solid particles that managed to be dragged along with the solvent, were filtered through a membrane filter. Dry extracts were obtained removing the organic solvent by vacuum using a Rotavapor. All extractions were performed in duplicate.

3.6.6. Carotenoids extraction

Freeze-dryed yeast biomass was ground in ball mill for 3 min at a frequency of 25 Hz using 5 cm diameter metal spheres. A quantity of 0.150 g was suspended in 2 mL DMSO in tin foil covered plastic test tubes (to prevent carotenoid degradation by exposure to light) containing acid-washed 425-600 µm glass beads (*Sigma*-Aldrich®). The suspension was stirred in a vortex mixer for 1 min and placed in a water bath at 55ºC for 1 h, followed by centrifugation for 10 min at 3900 rpm. These steps were repeated once and the supernatants transferred to a separatory funnel.

The pellet was ressuspended in 2 mL acetone and the extraction was carried out in the same way as with DMSO, and repeated several times until the pellet lost all its pigments and the acetone became colorless.

The acetone extract was mixed with the DMSO fraction and serial washed with 2 mL 20% NaCl solution at 5°C, 5 mL hexane or petroleum ether and 5-10 mL distilled water at 5ºC. The immiscible solvent mixture was vigorously shaken for about 30 seconds, releasing occasional accumulated vapor pressure inside the separation funnel until the colored (upper) phase became translucid. The two immiscible layers were then left to sit, after which the aqueous (bottom) phase was discarded and the organic fraction collected into a glass flask and evaporated under vacuum using a rotavapor (Buchi® R-200 Rotavapor with a R-490 Heating Bath and V-800 vacuum controller).

The dry extract was ressuspended in hexane and passed through cotton and anhydrous sodium sulfate in order to remove traces of water then evaporated under a gentle stream of nitrogen and resuspended in 3 mL filtered acetone. This step was performed twice.

a) Quantification by UV-VIS spectrophotometry

Absorption spectra of extracts were obtained in the visible radiation range (380-700 nm) using a spectrophotometer (Shimadzu UV-2401PC UV-VIS recording spectrophotometer).

TC were calculated by the Beer-Lambert law using an extinction coefficient corresponding to that of beta-carotene in acetone at a wavelength of 450 nm [ε = 2630 l / (10g.cm)].

b) Identification and quantification by HPLC

HPLC with a UV-VIS detector set to 450 nm was used to analyze the extracts. The system used consisted of a µ-Bondapack C18 reversed phase (250 x 4.0 mm) column with methanol [0.1% triethylamine (TEA)]: acetonitrile: ethyl acetate (75:15:10) as the mobile phase. Samples were eluted for 12 min at a flow rate of 0.8 mL.min^{-1}. Beta-carotene was identified by comparing retention times of the carotenoid in the sample

with the retention time of the standard (Sigma 97% β-carotene, United Kingdom). Standard solutions of β-carotene, with concentrations ranging from 0.06 to 6.5 μg.mL^{-1}, were used for the calibration curve (total β-carotene content (μg.mL-1) = Area x 0.003 + 0.0022) which was used to determine the total content of β-carotene. The identification of other carotenoids (torulene and torularhodin) was made by comparison of the chromatograms obtained with those reported in the literature for a similar system.

3.7. Kinetic Parameters

In order to characterize growth, lipid and carotenoid production of *R.toruloides*, several kinetic parameters were calculated.

3.7.1. Biomass productivity

Biomass productivity was calculated using the following equation:

$$Px = \frac{Xi - X0}{ti - t0}$$

Equation 3 - Biomass productivity [P_X ($g_{biomass}.L^{-1}.h^{-1}$)] in relation with t = 0h. Xi ($g.L^{-1}$)= biomass concentration at t = i; X0 ($g.L^{-1}$)= biomass concentration at t = 0h; ti = time at i (h); t0 = initial time (t = 0h)

3.7.2. Total fatty acid productivity and percentage

Total fatty acid productivity and percentage were calculated using the following equations, respectively:

$$PTFA = Px \times \frac{\%TFA\ (wTFA/Pwbiomass)}{100}$$

Equation 4 - Total fatty acid productivity [P_{TFA} ($g_{TFA}.L^{-1}.h^{-1}$)]. P_X = biomass productivity ($g_{biomass}.L^{-1}.h^{-1}$); %TFA ($w_{TFA}/w_{biomass}$) = percentage of Total Fatty Acids in relation to the biomass.

The %TFA was calculated according to the following equation:

$$\%FA\ (wTFA/wbiomass) = \frac{wFA}{wsample} \times 100$$

Equation 5 – Total fatty acid percentage [%TFA ($w_{tfa}/w_{biomass}$)]; mFA = total fatty acid amount (mg); msample = yeast biomass amount (mg).

3.7.3. Fatty acid composition

Fatty acid composition was calculated according to the following equation:

$$\%FAi\ (WFA/WTFA) = \frac{mFAi}{mTFA} \times 100$$

Equation 6 – Percentage of each fatty acid in total fatty acid weight. %FAi (P_{fa}/P_{tfa}) = percentage of fatty acid i; mFAi = fatty acid i weight (mg); mTFA = total fatty acid weight (mg), calculated by the sum of all fatty acids weights.

3.7.4. Total carotenoid productivity

TC productivity was calculated using the following equation:

$$PTC = Px \times CTC$$

Equation 7 - TC productivity [P_{TC} ($mg_{tc}.L^{-1}.h^{-1}$)]. Px = biomass productivity ($gbiomass.L^{-1}.h^{-1}$); C_{TC} = TC concentration ($mg_{carotenoids}.g_{biomass}^{-1}$).

3.8. Flow Cytometry

A flow cytometer (FACScalibur, Becton-Dickinson, Franklin Lakes, NJ, USA) equipped with an argon laser emitting at 488 nm and photomultipliers FL1 (530 ± 30 nm), FL2 (585 ± 42 nm), FL3 (> 670 nm) and FL4 (600 ± 16 nm) was used to monitor the cytoplasmic membrane integrity, mitochondrial and cytoplasmic membrane potentials, enzymatic activity and to quantify TC content in *R. toruloides* cells throughout the cultivations.

3.8.1. Plasma membrane integrity and mitochondrial potential

Cytoplasmic membrane integrity and potential were simultaneously monitored by fluorescence emitted by yeast cells double stained with the fluorochromes propidium iodide (PI) (Invitrogen, USA) and 3,3'-dihexyloxacarbocyanine iodide [$DiOC_6(3)$] (Invitrogen, USA), respectively.

PI is excluded by viable cells [**75**], as the stain passes through only damaged cell membranes, intercalating with the nucleic acids of injured and dead cells to form a bright red fluorescent complex [**76, 77**]. PI is excited at 536 nm and emits at 623 nm, so the fluorescence of cells stained with this fluorochrome can be detected both in FL2 and FL3 channels [**40**]. $DiOC_6(3)$ is a positively charged lipophilic carbocyanine stain that accumulates intracellularly in polarized or hyperpolarized cytoplasmic and mitochondrial membranes [**54**]. $DiOC_6(3)$ is excited at 484 nm and the fluorescence of the stained cells is measured at 501 nm may be detected in the FL1 channel [**40**].

Stock PI solution concentration was 1 $mg.mL^{-1}$ (in filtered milli-Q water) and final solution concentration in the cell suspension was 0.5 $\mu g.mL^{-1}$. DiOC6 (3) stock

solution concentration was 10 ng.mL^{-1} in DMSO, and the final solution concentration was 5 ng·mL^{-1}.

Samples taken throughout the trials were sonicated (Transsonic T 660/H, Elma, Germany) for 10 seconds to avoid cell aggregation, and diluted in phosphate buffer saline [PBS, pH 7.3 ± 0.2 (Oxoid, England)] in order to obtain about 800 to 1,000 events per second. Next, 0.5 µL $DiOC_6(3)$ were added to 499 µL diluted sample. The mixture was incubated in the dark at room temperature for 5 min, after which 0.5 µL IP were added and cells analysed immediately.

All buffers and Mili-Q water were filtered through 0.2 µm membrane filters (TPP Syringe filter 22**,** Switzerland and White nitrocellulose membrane filters, Filtres Fioroni, France, for buffer solutions and Mili-Q water, respectively)

Data obtained by multiparametric FC was analyzed in FCS Express 4 Flow Research Edition program.

3.8.2. At-line TC analysis

TC content was determined by measuring the autofluorescence of the yeast cells. To this end, we previously established a correlation between the autofluorescence of yeast cells read in the FL1, FL2 and FL3 channels and TC quantified by HPLC for the same samples. Since the content of carotenoids increases with the aging of the culture [**54**], the correlation was established by analyzing samples taken at different phases of cell growth. Thus, it is possible to correlate autofluorescence readings obtained by FC with the TC content through a linear regression [**54**].

The samples were sonicated (T Transsonic 660 / H, Elma, Germany) for 10 seconds to remove any cell aggregates and ensure individual analysis of cells. Next, the samples were diluted in phosphate buffer saline [PBS, pH 7.3 ± 0.2 (Oxoid, England)] in order to obtain between 800 and 1,000 events per second. Autofluorescence was then read for quantification of TC.

For the first sample, collected at the beginning of yeast growth, autofluorescence in the FL1, FL2 and FL3 channels was adjusted at the first logarithmic decade. This setting was used for subsequent readings made throughout the trials.

4. Results and discussion

4.1. Carotenoid quantification by HPLC

According to Freitas *et al.* (2014), the yeast cells autofluorescence can be used for at line detection of carotenoid content in yeasts, using FC [**54**]. However, the correlation described in that work, where *R. toruloides* NCYC 921 was cultivated in shake flasks, could not be used in the present work, because it was found that the biomass produced

in our bench bioreactor had a carotenoid composition different from the one observed in shake flasks. As a result, the yeast cells emitted fluorescence at different wave lengths when cultivated in different systems. Therefore, it was necessary to establish a new correlation between the TC content determined by the conventional method (extraction, and quantification of these compounds by HPLC), and the autofluorescence of cells measured by FC (see sections 3.6.6.and 3.8.2.).

Figure 2 shows the TC content and individual carotenoids (β-carotene, torulene, torularhodin) in $mg_{carotenoids}.g_{dry\ cell\ wieght}^{-1}$, determined by HPLC analysis of samples taken during assay I. Figure 3 displays the composition of carotenoids, in percentage.

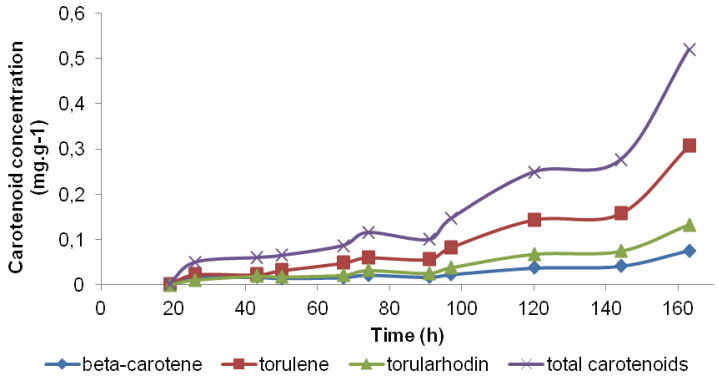

Figure 2. TC content and individual carotenoids (β-carotene, torulene, and torularhodin) in $mg_{carotenoids.glyophilized\ biomass}^{-1}$, determined by HPLC analysis of *R.toruloides* NCYC 921 biomass collected throughout assay I (section 4.2.1).

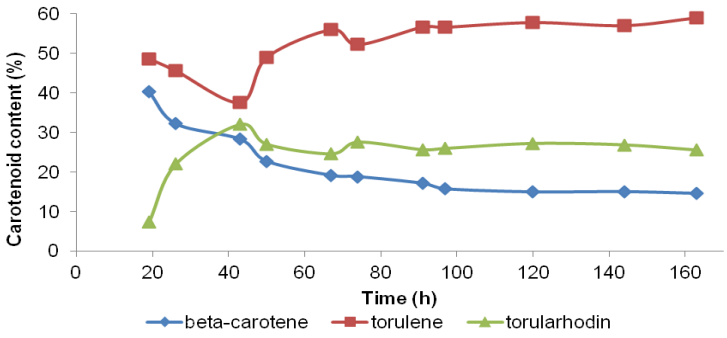

Figure 3. Carotenoid composition (percentage) in *R.toruloides* NCYC 921 biomass collected throughout assay I (section 4.2.1).

Through the analysis of Figures 2 and 3, it can be concluded that torulene was always the carotenoid produced in greater amounts, reaching a maximum of 59.00% of TC content (corresponding to 0.31 $mg.g^{-1}$). The percentage of β-carotene decreased during the assay. Initially, the yeast biomass contained 40.34% ($5x10^{-4}$ $mg.g^{-1}$) of β-carotene of TC content, and at the end reaches and stabilizes at 14.50% (0.08 $mg.g^{-1}$). Torularhodin percentage increased, reaching a maximum at t = 43 h with 31.95% (0.02 $mg.g^{-1}$) and decreases slightly to the end of the test, ending at 25.55% (0.13 $mg.g^{-1}$).

4.1.1. Autofluorescence measured by FC

The autofluorescence of *R. toruloides* cells detected in FL1, FL2 and FL3 channels show similar profiles, with higher autofluorescence values observed in the FL2 channel, as is evident in Figure 4.

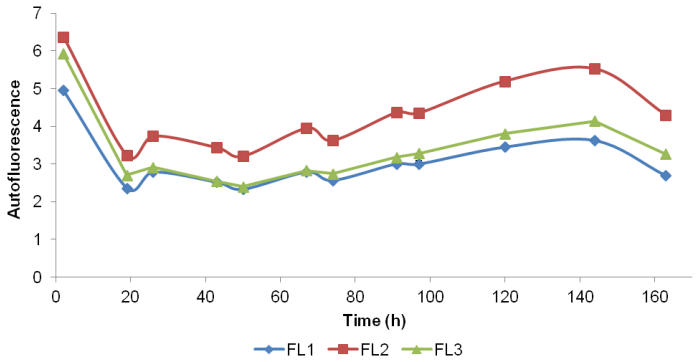

Figure 4. Autofluorescence of *R. toruloides* cells detected in FL1, FL2 and FL3 channels, throughout assay I (section 4.2.1).

4.1.2. Correlation between autofluorescence and TC

Correlations were calculated for each autofluorescence measured in FL1, FL2 and FL3 channels versus TC content. The best correlation was found for TC content versus autofluorescence detected in the FL2 channel (Figure 5).

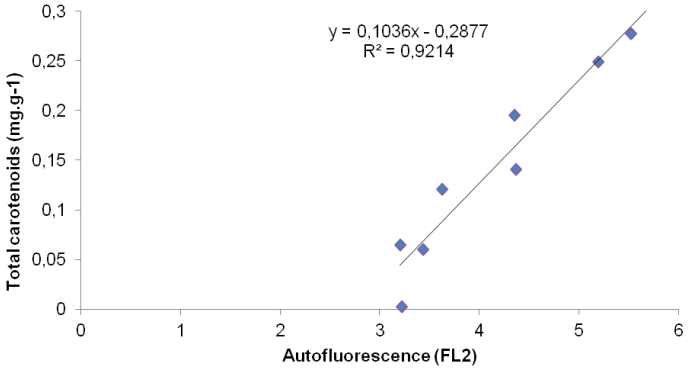

Figure 5. Correlation for the TC content in $mg.g^{-1}$ assessed by HPLC, versus the yeast cells autofluorescence detected in the FL2 channel, determined from samples taken during the r assay I (section 4.2.1).

This correlation was used to convert the autofluorescence readings of *R. toruloides* cells during the time course of the fed-batch cultivations, to determine TC content for all assays.

4.2. Yeast fed-batch cultivations

All assays were performed in a bench reactor, operated in fed-batch mode, with the objective of maximizing yeast cell growth and lipids and carotenoids accumulation.

The conditions used are summarized in table 3.

Table 3. Cultivation conditions used for assays I-IV using *R. toruloides* cells.

Assay	System	pH	Feed system	Added solutions	Speed rate
I	Fed-Batch	5.5	Peristaltic pump	Nutrients + glucose (NG) and Glucose (G) 600 $g.L^{-1}$	600 rpm
II	Fed-Batch	4.0	Peristaltic pump	Nutrients + glucose and Glucose 600 $g.L^{-1}$	Depending on DO
III	Fed-Batch	4.0 (active growth phase) – 5.0 (product accumulation phase)	Peristaltic pump	Nutrients + glucose and Glucose 600 $g.L^{-1}$	Depending on DO
IV	Fed-Batch (two impellers)	4.0 (active growth phase) – 5.0 (product accumulation phase)	Peristaltic pump	Nutrients + glucose and Glucose 600 $g.L^{-1}$	Depending on DO

4.2.1. Assay I

Figure 6 shows the biomass concentration, OD, biomass productivity, the natural logarithm of the biomass, DO, stirring rate, residual glucose and nitrogen concentrations, fatty acid percentage and productivity, TC concentration and productivity profiles obtained for this assay.

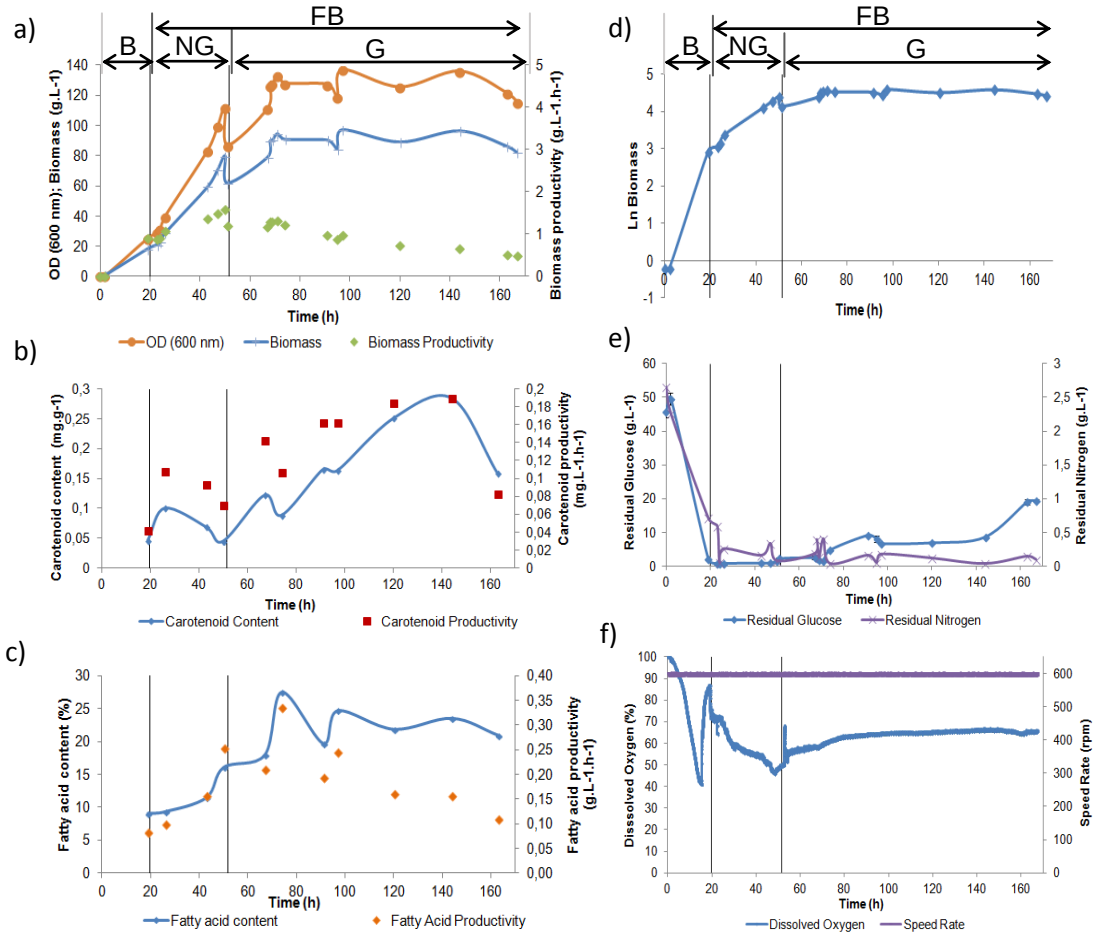

Figure 6. *R. toruloides* yeast growth in a fed-batch system with addition of a nutrient solution with glucose, yeast extract and magnesium sulphate (solution NG), and concentrated glucose solution (solution G) via a peristaltic pump, at pH 5.5 (Assay I): **a)** Optical density (OD), yeast biomass concentration in $g.L^{-1}$ and productivity in $g.L^{-1}.h^{-1}$. The OD and biomass concentration values are the average of at least two replicates with a standard deviation of less than 10% (n = 2); **b)** TC concentration in $mg.L^{-1}$ and carotenoids productivity in $mg.L^{-1}.h^{-1}$; **c)** Fatty acid percentage and fatty acid productivity in $g.L\text{-}1.h^{-1}$. Fatty acid data represent the mean of four determinations (two independent samples injected twice with a standard deviation of less than 10% (n = 4); **d)** Natural logarithm profile; **e)** Residual glucose and nitrogen concentrations profiles in $g.L^{-1}$. Values are the average of at least three replicates with a standard deviation of less than 10% (n = 2); **f)** Dissolved oxygen **(**DO) percentage and bioreactor speed rate in rpm.
B = batch phase; FB = fed-batch phase; NG = nutrients with glucose solution; G = concentrated (600 $g.L^{-1}$) glucose solution.

The addition of solution NG intended to extend the yeast's active growth phase, obtaining a specific growth rate of 0.05 h^{-1} (R^2 = 0.99) for that time period (Figure 6d).

Supply of solution NG began at t = 19.67 h, when the residual glucose concentration was low (2.01 $g.L^{-1}$) (Figure 6e). Solution G was added from t = 51.50 h onwards.

The culture reached the stationary phase 51.00 h after inoculation, with a biomass concentration of 61.87 g L^{-1} corresponding to 87 OD, and a biomass productivity of 1.20 $g.L^{-1}.h^{-1}$ (Figure 6a).

The maximum biomass concentration corresponded to 97.18 $g.L^{-1}$ obtained at t = 97 h, with a biomass productivity of 0.99 $gL^{-1}.h^{-1}$ and 137 optical density (OD). The highest biomass productivity was reached at 50.00 h (1.58 $gL^{-1}.h^{-1}$) with a biomass concentration of 79.76 $g.L^{-1}$ (Figure 6a).

During yeast growth, DO was maintained at values higher than 40% (Figure 6f) in order to avoid growth limitations due to oxygen deficiency. DO values decreased from 100% to close to 40%, when it rose again close to 87% due to depletion of the carbon source. During the addition of solution NG, DO dropped to values close to 50%, indicative of cellular metabolic activity. Once solution G was added, DO values remained around 65%. During addition of solution G, there was an increase in TC and fatty acid production, although the TC content increase occurred later than the fatty acid content increase (Figures 6b and 6c).

Stirring rate was maintained at 600 rpm throughout the trial (Figure 6f). Residual nitrogen levels decreased from 2.65 $g.L^{-1}$ to values close to zero up to t = 20.00 h and remained below 0.2 $g.L^{-1}$ throughout the addition of solutions NG and G (t > 19.67 h) (Figure 6e).

In this assay, the profile of residual glucose followed the same trend of the residual nitrogen profile, although the glucose concentration increased at the end of the test (Figure 6e) suggesting that, at the time, the metabolic activity of the cells diminished due to exhaustion of a nutrient other than nitrogen, as the cells maintain their activity when this nutrient is not present. The feed rates of the NG and G solutions were adjusted to maintain the residual glucose levels below 40 $g.L^{-1}$ in order to avoid yeast growth inhibition by the substrate and, at the same time, avoiding the lack of carbon in the cells.

Production of fatty acids followed the biomass profile, peaking at the beginning of the stationary phase and decreasing at the end of the test, at 167.00 h (Figure 6c). The maximum fatty acid percentage was obtained at 74.00 h corresponding to 27.57% (w/w) in relation to the dry cell weight. The maximum fatty acids productivity was obtained at 74.00 h, with a value of 0.34 $g.L^{-1}.h^{-1}$, decreasing until the end of the experiment as a result of the decrease in the fatty acid content and biomass productivity during stationary phase (Figures 6a and 6c).

Carotenoids synthesis began during the stationary phase, when solution G was added to the culture (t = 51.50 h) supplying the carbon necessary for the production of storage materials, since the glucose medium was exhausted before this addition. TC content and productivity reached their maximums at t = 144.00 h with 0.28 $mg.g^{-1}$ and 0.191 $mg.L^{-1}.h^{-1}$, respectively. (Figure 6b).

Figure 7 shows the fatty acid composition obtained during this assay.

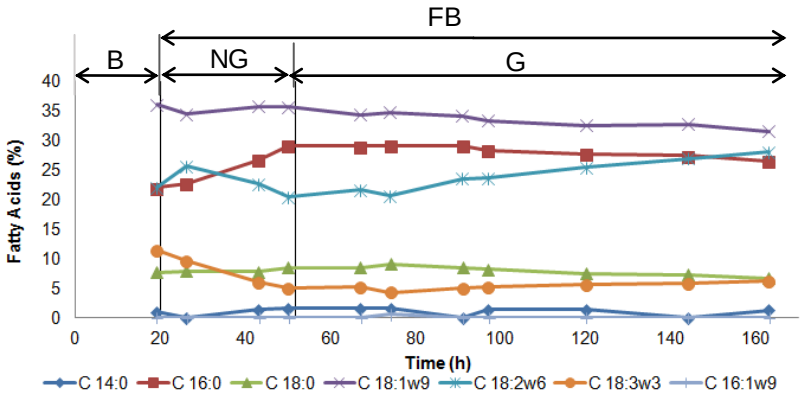

Figure 7. *R. toruloides* Fatty acid composition during assay I, at pH 5.5. The data represent the mean of four determinations (two independent samples injected twice) with a standard deviation lower than 10% (n = 4).
B = batch phase; FB = fed-batch phase; NG = nutrients with glucose solution; G = concentrated (600 $g.L^{-1}$) glucose solution.

The dominant fatty acids were oleic (18:1ω9), palmitic (16:0), linoleic (18:2ω6) and stearic (18:0) acids. The proportions of these fatty acids are in the range of those published by Sawangkeaw *et al.* (2013) [**78**] for the same yeast with the exception of palmitic acid (16:0), which presents with higher percentages (16:0: 13-16%; 18:0: 4-41% , 18:1ω9: 18-42% and 18:2ω6: 15-29%).

At the end of the cultivation (t = 163.00 h), oleic acid (18:1ω9) was in larger quantity with 31.48% of the total fatty acid content, followed by linoleic (18:2ω6), palmitic (16:0) and stearic (18:0), with values of 27.48%, 26.40% and 6.62%, respectively. After the addition of solution G (t = 51.50 h), the percentages of oleic acid (18:1ω9), palmitic acid (16:0) and stearic acid (18:0) decreased slightly until the end of the experiment (from 34.33% to 31.48%, from 28.95% to 26.40% and from 8.45% to 6.62%, respectively), whereas the percentage of linoleic acid (18:2ω6) increased from 21.59 % to 27.97%.

Myristic acid (14:0) varied between 0 and 1.57% throughout the experiment and linolenic acid (18:3ω3) between 4.32% and 11.41%. Palmitoleic acid (16:1ω9) acid was detected in smaller quantities only at 74.00 h with a total content of 0.70%.

According to the European standard EN 14214 (European Standard that describes the requirements and test methods for biodiesel) [**79**], due to linolenic (18:3ω3) acid's propensity to oxidize [**80**] its presence is restricted to percentages below 12% and

maximum polyunsaturated fatty acids with four or more double bonds are limited to 1%. The results displayed in Figure 7 show that the *R. toruloides* fatty acid composition meets the European standard requirements.

Figure 8 shows the percentage of saturated fatty acids (SFA) monounsaturated fatty acids (MUFA) and polyunsaturated fatty acids (PUFA) throughout this assay.

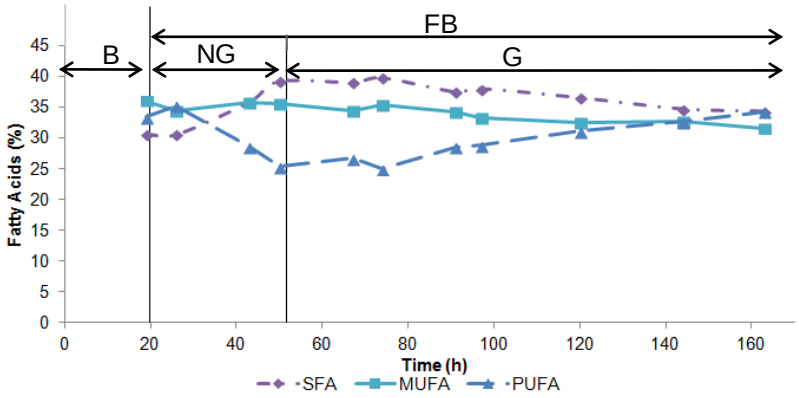

Figure 8. Composition of saturated fatty acids (SFA) monounsaturated fatty acids (MUFA) and polyunsaturated fatty acids (PUFA) obtained in assay I for *R. toruloides*, at pH 5.5.
B = batch phase; FB = fed-batch phase; NG = nutrients with glucose solution; G = concentrated (600 $g.L^{-1}$) glucose solution.

SFA are in greater proportion with a maximum at t = 74.00 h corresponding to 39.68%, followed by MUFA with a maximum at t = 19.00 h corresponding to 35.99%, and finally the PUFA, with a maximum at t = 26.00 h corresponding to 35.17%.

SFA increased during the addition of solution NG (from 30.61% to 39.11%), continuing to rise during the addition of solution G up to 74 h, and then decreasing until the end of the test (34.30%).

PUFA have the opposite behavior of SFA, decreasing during the addition of solution NG (from 33.40% to 25.32%) and increased during the addition of solution G to the end of the test (34.21%).

MUFA remain approximately constant during the addition of solution NG (ranging from 35.99% to 35.57%), decreasing during the addition of solution G to the end of the trial (31.48%).

At the end of the assay, percentages are close to each other (34.30% for SFA, 31.48% for MUFA and 34.21% for PUFA).

4.2.2. Assay II

Contrary to the works published by Pan et al. (1986) [**69**], parallel studies within our project concluded that the optimum pH for *R. toruloides* biomass production is 4.0 and not 5.5 (unpublished results).

We therefore carried out this second assay at pH 4.0 with the aim of increasing *R. toruloides* biomass productivity since this is closely related to the products productivity in the study. The other conditions were the same as the previous assay.

Figure 9 shows the profiles of the biomass concentration, OD, biomass productivity, the natural logarithm of the biomass, DO, stirring rate, residual glucose and nitrogen concentrations, fatty acid percentage and productivity, TC concentration and productivity for this assay.

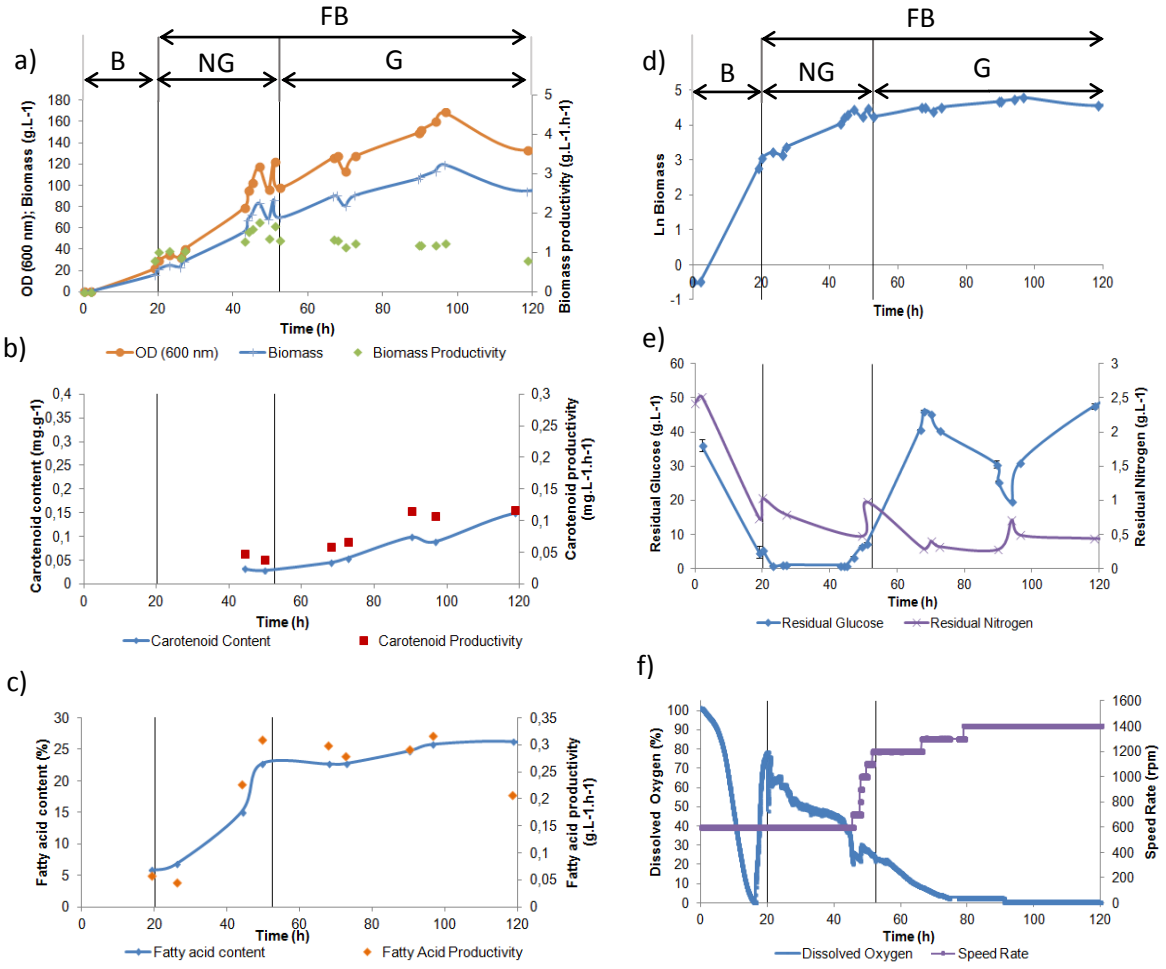

Figure 9. *R. toruloides* yeast growth in a fed-batch system with addition of a nutrient solution with glucose, yeast extract and magnesium sulphate, and concentrated glucose solution via a peristaltic pump, at pH 4.0 (Assay II): **a)** Optical density (OD), yeast biomass concentration in $g.L^{-1}$ and productivity in $g.L^{-1}.h^{-1}$. The OD and biomass concentration values are the average of at least two replicates with a standard deviation of less than 10% (n = 2); **b)** TC concentration in $mg.L^{-1}$ and carotenoids productivity in $mg.L^{-1}.h^{-1}$; **c)** Fatty acid percentage and fatty acid productivity in $g.L^{-1}h^{-1}$. Fatty acid data represent the mean of four determinations (two independent samples injected twice with a standard deviation of less than 10% (n = 4); **d)** Natural logarithm profile; **e)** Residual glucose and nitrogen concentrations profiles in $g.L^{-1}$. Values are the

average ay least 3 replicates with a standard deviation of less than 10% (n = 2); **f)** DO and bioreactor speed rate in rpm.
B = batch phase; FB = fed-batch phase; NG = nutrients with glucose solution; G = concentrated (600 $g.L^{-1}$) glucose solution.

The addition of solution NG extended the yeast's active growth phase, with a specific growth rate of 0.05 h^{-1} (R^2 = 0.98) for the NG addition phase (Figure 9d).

Addition of NG solution to the bioreactor started at 20.08 h when residual glucose concentration levels were low (5.62 $g.L^{-1}$) (Figure 9e). Solution G was added to the bioreactor at t = 52.58 h.

The culture entered the stationary phase at t = 52.50 h with a biomass concentration of 69.64 $g.L^{-1}$ corresponding to 98 OD and a biomass productivity of 1.31 $g.L^{-1}.h^{-1}$ (Figure 9a).

The maximum biomass concentration was 119.61 $g.L^{-1}$ at t = 96.5 h with a biomass productivity of 1.23 $g.L^{-1}.h^{-1}$ and 168.8 OD (Figure 9a).

The maximum biomass productivity was reached at t = 47.00 h (1.76 $g.L^{-1}.h^{-1}$) with a biomass concentration of 83.48 $g.L^{-1}$ (Figure 9a).

As expected, changing the pH to 4.0 resulted in a maximum biomass concentration increase to 119.61 $g.L^{-1}$. This increase in biomass concentration resulted in an increased oxygen consumption, with levels initially dropping from 100% to values close to 0.5%, when it began to rise again to a value near 79% due to the depletion of the carbon source (Figure 9f). During the addition of solution NG, DO values decreased to 23% (t = 52.58 h) indicating cellular metabolic activity. After addition of solution G, DO values continued to decrease until it remained in the 1-4% range (Figure 9f).

The stirring rate was maintained at 600 rpm until t = 45.50 h, when the DO level was 21% (Figure 9f). From this point onward, the air flow was increased to 3 $L.min^{-1}$ and the bioreactor was set to an automatic input so that the stirring rate would automatically increase whenever DO values decreased below 40%, in order to keep the percentage above this threshold, to prevent oxygen limitation. From t = 79 h, the stirring rate remained at 1400 rpm until the end of the trial. Unfortunately, DO levels kept decreasing and stabilized at a very low percentage, thus unable to ensure oxygen sufficient conditions to the yeast cells, as it can be seen in figure 9f.

Residual nitrogen levels decreased from 2.43 $g.L^{-1}$ to 1.03 $g.L^{-1}$ up to t = 20.00 h, decreasing throughout the addition of solution NG and increasing slightly until t = 51 h (0.98 $g.L^{-1}$), right at the end of the addition of solution NG. Residual nitrogen concentration decreased once more after adding solution G and remained below 0.5 $g.L^{-1}$ during the entire assay with the exception of t = 94 h with a nitrogen concentration of 0.72 $g.L^{-1}$ (Figure 9e).

Residual glucose levels decreased from 56.33 $g.L^{-1}$ to 5.62 $g.L^{-1}$ during the batch phase (Figure 9e). During the addition of solution NG, from t = 23 h to t = 43 h, glucose concentration remained in the 2.16-2.72 $g.L^{-1}$ range after which the peristaltic pump rate was increased resulting in increasing glucose concentration levels, reaching 7.17 $g.L^{-1}$ at the end of solution NG addition (Figure 9e). After switching to solution G, concentration levels increased steadily and the pump rate was decreased to 0.4 rpm at t = 67.75 h and to 0.2 rpm shortly after (t = 70 h) (not shown) to prevent glucose concentration from exceeding 40 $g.L^{-1}$ and consequential substrate inhibition.

However, residual glucose concentration exceeded 40 $g.L^{-1}$ after t = 66.75 h and at the end of the assay (Figure 9e). This can be attributed to the fact that the peristaltic pump feed rate should have been set at a lower speed rate than 0.3 rpm from 94 h onwards, in order to prevent glucose accumulation in the medium thus substrate growth inhibition. This factor, coupled with the lack of oxygen during the remaining hours of the assay (Figure 9f) and suspicions that the glucose test strips stopped giving accurate qualitative estimates up to a certain concentration, resulted in the accumulation of glucose in the culture medium above the desired values.

The accumulation of fatty acids follows the same profile of biomass concentration up to the stationary phase (Figures 9a and 9c) and slightly increased during the addition of solution G. The maximum total fatty acid content in the stationary phase was obtained at t = 117.67 h corresponding to 26.19% relative to the biomass (Figure 9c). The highest fatty acid productivity was obtained at t = 96.5 h corresponding to 0.32 g $L^{-1}.h^{-1}$. While the total fatty acid content remained stable until the end of the assay (25-26%) fatty acid productivity decreased along with biomass productivity (Figures 9a and 9c).

As in the previous assay, carotenoids began to be accumulated when solution G was added to the culture during the stationary phase (t = 52.58 h) (Figure 9b). TC content increased throughout the cultivation, especially during the stationary phase, peaking at the end of the test with 0.15 $mg.g^{-1}$.

Figure 10 shows the fatty acids composition obtained during this assay.

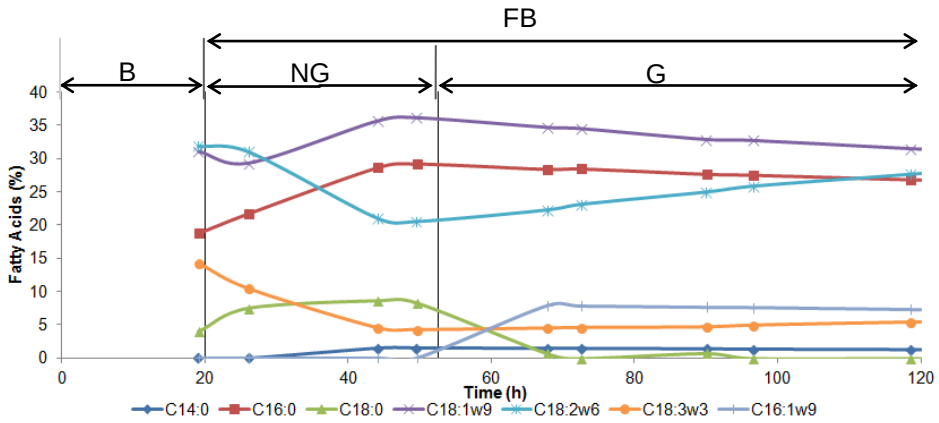

Figure 10. Fatty acid composition percentage obtained in assay II for *R. toruloides* with addition of nutrients with glucose and concentrated glucose solutions via peristaltic pump, at pH 4.0. The data represent the mean of four determinations (two independent samples injected twice) with a standard deviation lower than 10% (n = 4).
B = batch phase; FB = fed-batch phase; NG = nutrients with glucose solution; G = concentrated (600 $g.L^{-1}$) glucose solution.

Oleic (18:1ω9), palmitic (16:0) and linoleic (18:2ω6) acids were dominant.

The percentages of oleic acid (18:1ω9) are in the range of those published by Sawangkeaw *et al*. (2013) [**78**] for *R. toruloides* (18:1ω9: 18-42%). As in assay I, the proportion of palmitic acid (16:0) was higher than the values reported by these authors (16:0: 13-16%). Linoleic acid (18:2ω6) percentages are in the range of published values (18:2ω6: 15-29%) with the exception of t = 19.00 h and t = 26.00 h, with slightly higher percentages.

At the end of the assay (t = 118.5 h), oleic acid (18: 1ω9) presented a higher percentage (31.48%) of total fatty acids, followed by linoleic (18: 2ω6) and palmitic (16:0) acids with 27.65% and 26.82%, respectively.

The percentages of oleic (18:1ω9) and palmitic acid (16:0) increased until the addition of the solution G (t = 52.58 h), from 31.07% to 36.13% and 18.72% to 29.19%, respectively. After addition of solution G, the proportion of both fatty acids decreased by the end of the test (t = 118.5 h) to 31.48% and 26.82%, respectively.

Linoleic (18: 2ω6) and linolenic acid (18:3ω3) showed the opposite profile, decreasing during the addition of solution NG (from 31.88% to 20.56% and 14.31% to 4.33%, respectively) and then increased until the end of the assay (to 27.65% and to 5.45%, respectively).

Stearic acid (18:0) was detected with percentages lower than 10%, increasing from 4.02% to 8.27% until the addition of solution G. After the addition, the proportion of stearic acid (18:0) decreased reaching values lower than 1% and was not detected at the end of the assay. The percentages of stearic acid (18:0) are in the range of values published values Sawangkeaw *et al*. (2013) before adding solution G. After addition, the

acid can be found with lower values than those reported by these authors (18: 0: 4-41%).

Myristic acid (14:0) and palmitoleic acid (16:1ω9) reached 1.52% and 7.91%, respectively, at t = 67.67 h, values which are not present in yeast biomass obtained during assay I at pH 5.5 and are in accordance with Jeenor *et al*. (2006) [**81**] who state that oxygen limited conditions modifies the activity of elongases, enzymes involved in the synthesis of long chain fatty acids..

Linolenic acid (18: 3ω3) percentage was below 12%, except at t = 19.00 h with 14.31%. No polyunsaturated fatty acids with four or more double bonds were detected. Therefore, the yeast biomass fatty acids profile for this assay fulfills the European standard requirements.

Figure 11 shows the percentage of saturated fatty acids (SFA) monounsaturated fatty acids (MUFA) and polyunsaturated fatty acids (PUFA) throughout this assay.

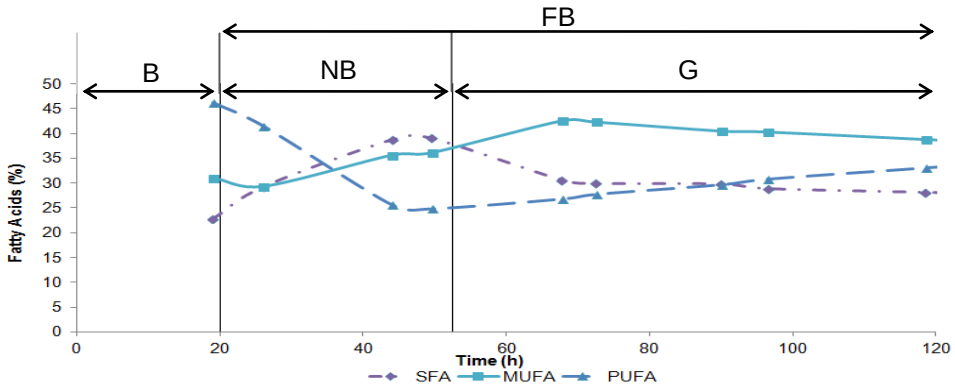

Figure 11. Composition of saturated fatty acids (SFA) monounsaturated fatty acids (MUFA) and polyunsaturated fatty acids (PUFA) obtained in assay II for *R. toruloides* with addition of nutrients with glucose and concentrated glucose solutions via peristaltic pump, at pH 4.0.

At the end of the assay, MUFA present the highest percentage (38.81%), followed by PUFA and SFA with 33.10% 28.09%, respectively. MUFA have a maximum at t = 67.75 h with 42.59%, PUFA at t = 19.00 h with 46.19% and SFA at t = 49.50 h corresponding to 38.98%.

MUFA ranged between 31.07% and 42.59% throughout the assay, increasing from 29.29% to 36.13% during the addition of solution NG. MUFA continued to increase during the addition of solution G until t = 67.75 h (42.59%), decreasing to the end of the assay (38.81%).

SFA ranged between 22.74% and 38.98% throughout the test, increasing during the addition of solution NG (from 22.74% to 38.98%) and decreasing during the addition of solution G until the end of the assay (28.09%).

PUFA ranged between 24.89% and 46.19% throughout the test, exhibiting the opposite profile of MUFA and SFA, decreasing during the addition of solution NG (from 46.19% to 24.89%) and increasing until the end of the experiment to 33.10%.

4.2.3. Assay III

Despite problems from oxygen deprivation, the results from assay II confirmed that the optimum pH for the production of yeast biomass is 4.0. The same parallel studies that led to this conclusion also revealed that the optimum pH for carotenoids and fatty acids production by *R.toruloides* is 5.0 (unpublished results).

In this assay, we used the same system and feeding strategy used in assays I and II.

In this assay, we adjusted the pH to 4.0 during the yeast's growth phase and, once the culture reached the stationary phase, at which growth cell division slows down, we adjusted the pH of the culture medium to 5.0 to promote the accumulation of lipidic storage products such as carotenoids. In this assay we set the speed rate depending on the DO readings, so that above the threshold of 40% DO the speed rate increased in order to increase the k_La (volumetric oxygen transfer coefficient) thus the oxygen availability in the system. The air inflow was also increased.

Figure 12 shows the profiles of the biomass concentration, OD, biomass productivity, the natural logarithm of the biomass, DO, stirring rate, residual glucose and nitrogen concentrations, fatty acid percentage and productivity, TC concentration and productivity for this assay.

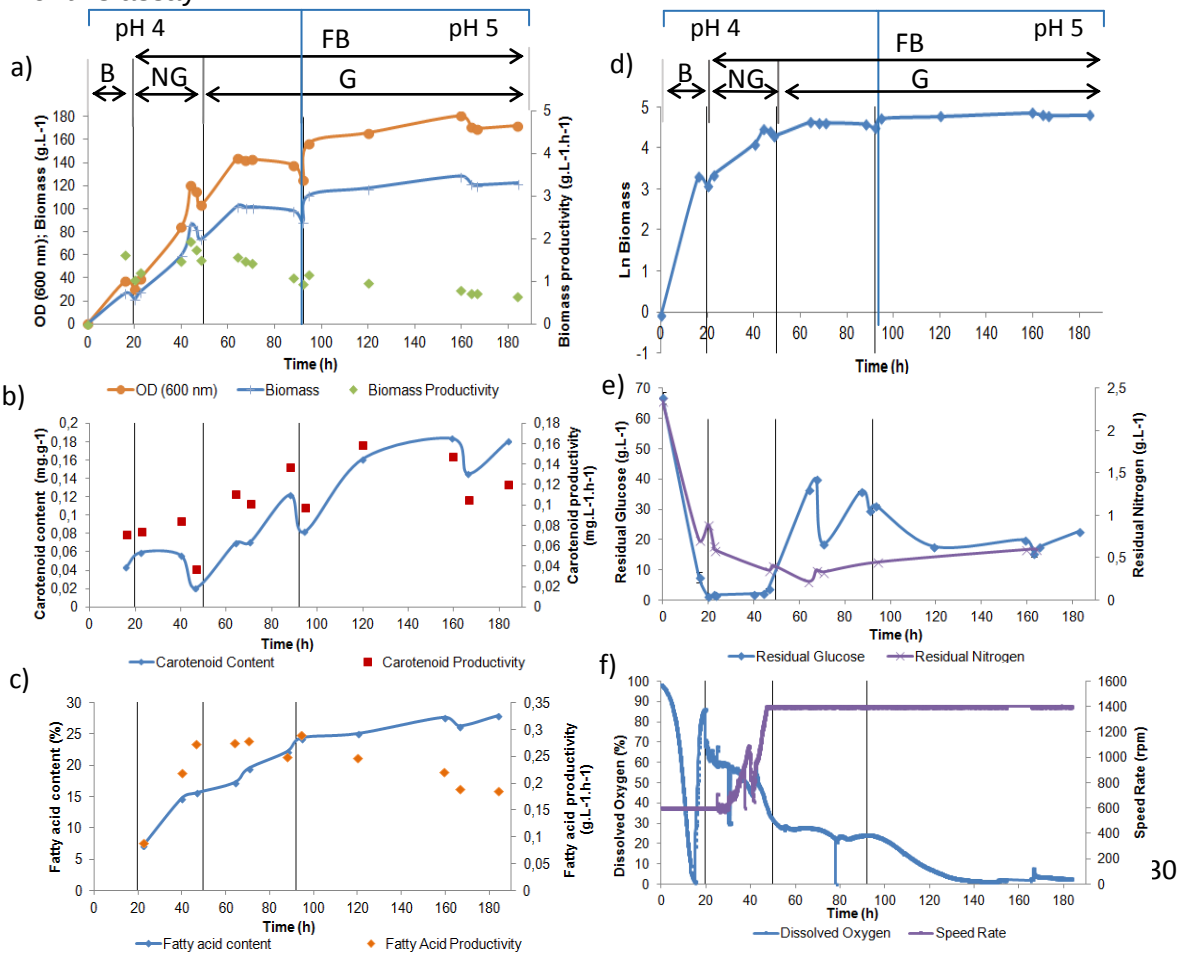

Figure 12. *R. toruloides* yeast growth in a fed-batch system with addition of a nutrient solution with glucose, yeast extract and magnesium sulphate, and concentrated glucose solution via a peristaltic pump, at pH 4.0 and 5.0 (Assay III): **a)** Optical density (OD), yeast biomass concentration in $g.L^{-1}$ and productivity in $g.L^{-1}.h^{-1}$. The OD and biomass concentration values are the average of at least two replicates with a standard deviation of less than 10% (n = 2); **b)** TC concentration in $mg.L^{-1}$ and carotenoids productivity in $mg.L^{-1}.h^{-1}$; **c)** Fatty acid percentage and fatty acid productivity in $g.L^{-1}h^{-1}$. Fatty acid data represent the mean of four determinations (two independent samples injected twice with a standard deviation of less than 10% (n = 4); **d)** Natural logarithm profile; **e)** Residual glucose and nitrogen concentrations profiles in $g.L^{-1}$. Values are the average of the replicates with a standard deviation of less than 10% (n = 2); **f)** DO and bioreactor speed rate in rpm.
B = batch phase; FB = fed-batch phase; NG = nutrients with glucose solution; G = concentrated (600 $g.L^{-1}$) glucose solution.

The addition of solution NG extended the yeast's active growth phase, with a specific growth rate of 0.05 h^{-1} (R^2 = 0.93) for the NG addition phase (Figure 12d).

Addition of solution NG began at 19.5 h when residual glucose concentration levels were low (1.23 $g.L^{-1}$) (Figure 12e). Solution G was added to the bioreactor at t = 49.5 h. The pH was changed from 4.0 to 5.0 at t = 92 h.

The culture entered the stationary phase at t = 64 h with a biomass concentration of 102 $g.L^{-1}$ corresponding to 144.5 OD and a biomass productivity of 1.59 $gL^{-1}.h^{-1}$ (Figure 12a).

The maximum biomass concentration was 128.26 $g.L^{-1}$ at t = 159 h with a biomass yield of 0.80 $g.L^{-1}.h^{-1}$ and 181 OD (Figure 12a).

The maximum biomass productivity was reached at t = 44.00 h (1.94 $g.L^{-1}.h^{-1}$) with a biomass concentration of 86.06 $g.L^{-1}$ (Figure 12a).

The glucose added to the pre-inoculum was consumed as shown by the DO profile dropping from 100% to levels close to zero then increasing to 86.25% right before adding solution NG (Figure 12f). Feeding the bioreactor with solution NG (from t = 19.5 to t = 46.5 h) decreased DO levels once again due to yeast cells' metabolic activity. From t = 46.5 h to the end of the assay, the same problem from the previous assay occurred, with oxygen levels dropping and staying below 40% (Figure 12f).

Residual nitrogen levels decreased from 2.34 $g.L^{-1}$ to 0.89 $g.L^{-1}$ up to t = 20.00 h, decreasing throughout the addition of NG and G solutions until t = 67.5 h when it started to increase until t = 164 h to 0.60 $g.L^{-1}$ (Figure 12e). This increase was due to inaccurate ammonia titrations when determining residual nitrogen.

Residual glucose levels decreased from 66.81 $g.L^{-1}$ to 1.23 $g.L^{-1}$ during the batch phase, remaining in the 1.23-3.69 $g.L^{-1}$ range from t = 20 h to t = 46.5 h (Figure 12e). When solution G was added, the residual glucose concentration attained 40 $g.L^{-1}$ at t = 67.5 h. At this time, the pump speed rate was decreased to 0.3 rpm, after which residual glucose concentration decreased to 18.48 $g.L^{-1}$ at t = 70.5 h, increasing again to a concentration level close to 40 $g.L^{-1}$ (35.70 $g.L^{-1}$) at t = 87 h. Decreasing the pump's speed rate to 0.2 rpm (not shown) managed to keep residual glucose concentration

below 40 $g.L^{-1}$ until the end of the cultivation (Figure 12e). It is worth noting that at t = 92 h, when the pH in the bioreactor was changed to 5.0, glucose levels decreased. When analyzing figure 12b, one can see that even though carotenoid accumulation began after supplying the yeast cells with the concentrated glucose solution, it increased even further after the pH changed, reaching a peak at t = 159.5 h with 0.18 $mg.g^{-1}$. This peak value was higher than the previous assay, the same as observed with the maximum carotenoid productivity (0.16 $mg.L^{-1}h^{-1}$ at t = 120 h). Fatty acids also show an increase after the pH change, reaching a peak at t = 183 h with 27.88%. Although fatty acid productivity was lower (0.29 $g.L^{-1}h^{-1}$) than in assay II, the maximum productivity in this assay was reached earlier and also after the pH change (t = 93.50 h). The aforementioned results are consistent with our conclusions that pH 5.0 is the optimum value for the production of carotenoids and fatty acids.

Figure 13 shows the fatty acids composition obtained during this assay.

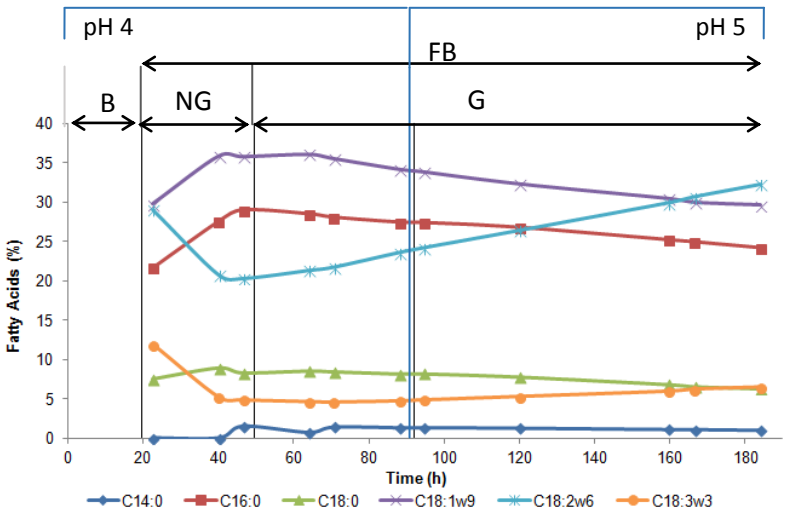

Figure 13. Fatty acid composition percentage obtained in assay III carried out at pH 4.0 and 5.0. The data represent the mean of four determinations (two independent samples injected twice) with a standard deviation lower than 10% (n = 4).
B = batch phase; FB = fed-batch phase; NG = nutrients with glucose solution; G = concentrated (600 $g.L^{-1}$) glucose solution.

Like in the two previous assays, oleic (18:1ω9), palmitic (16:0) and linoleic (18:2ω6) acids were the most prevalent fatty acids.

Once again, oleic acid (18:1ω9) presents percentages consistent with those published by Sawangkeaw *et al*. (2013) [**78**] for *R. toruloides* (18:1ω9: 18-42%). As in assay I and II, the proportion of palmitic acid (16:0) was higher than the values reported by these authors (16:0: 13-16%). Linoleic acid (18:2ω6) percentages are in the range of published values (18:2ω6: 15-29%) with the exception of t ≥ 159.5 h.

At the end of the assay (t = 184 h), linoleic acid (18:2ω6) presented a higher percentage (32.29%) of total fatty acids, followed by oleic (18:1ω9) and palmitic (16:0) with 29.61% and 24.24%, respectively.

Oleic acid (18:1ω9) percentage increased until the pump's speed rate was adjusted to 0.8 rpm (not shown), from 29.78% to 35.93%.

Palmitic acid (16:0) increased until the addition of the concentrated glucose solution (t = 49.5) from 21.69% to 29.00%. After supplying the culture medium with the concentrated glucose solution, the proportion of both fatty acids decreased to the end of the test (t = 187 h).

Linoleic (18:2ω6) and linolenic acid (18:3ω3) showed the opposite profile, decreasing during the addition of solution NG (from 29.05% to 20.33% and 11.89% to 4.90%, respectively) and increased until the end of the assay (to 32.29% and to 6.52%, respectively).

The percentages of stearic acid (18:0) remain somewhat stable throughout the whole assay and are in the range of values published by Sawangkeaw *et al*. (2013) [**78**].

Palmitoleic acid (16:1ω9) was not detected in this assay.

Linolenic acid (18:3ω3) stayed below 12% and no polyunsaturated fatty acids with four or more double bonds were detected, therefore R. toruloides fatty acids for this assay also fulfill the European standard requirements.

Figure 14 shows the percentage of saturated fatty acids (SFA) monounsaturated fatty acids (MUFA) and polyunsaturated fatty acids (PUFA) for this assay.

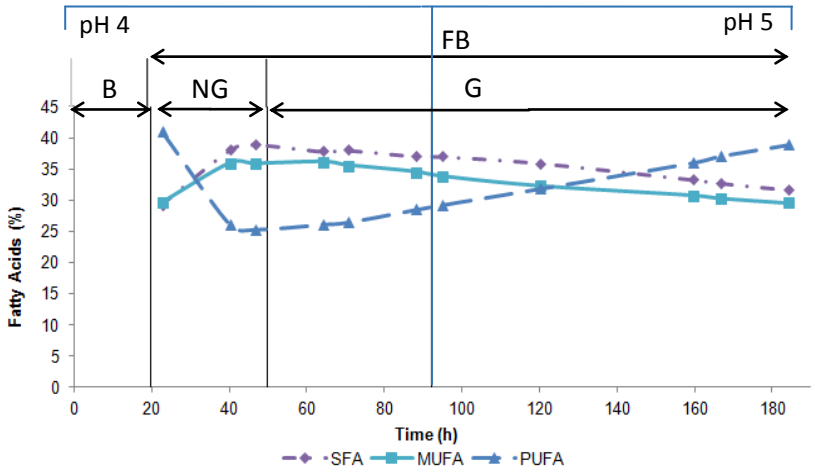

Figure 14. Composition of saturated fatty acids (SFA), monounsaturated fatty acids (MUFA) and polyunsaturated fatty acids (PUFA) obtained in assay III for *R. toruloides* with addition of nutrients with glucose and concentrated glucose solutions via peristaltic pump, at pH 4.0 - 5.0.
B = batch phase; FB = fed-batch phase; NG = nutrients with glucose solution; G = concentrated (600 $g.L^{-1}$) glucose solution.

At the end of the assay, PUFA present the highest percentage (38.82%), followed by SFA and MUFA with 31.57% and 29.62%, respectively. PUFA have a maximum at t = 19

h with 40.95%, MUFA at t = 40 h with 35.93% and SFA at t = 46.5 h corresponding to 38.92%.

SFA and MUFA show very similar patterns and close percentages, both increasing during the addition of solution NG (with the exception of MUFA from t = 40 h to t = 46.5 h) and decreasing during the addition of the concentrated glucose solution (with the exception of MUFA from t = 46.5 h to t = 64 h) until the end of the assay.

Just as in the previous assay, PUFA decreased during the addition of solution NG (from 40.95% to 25.23%) and increasing until the end of the assay to 38.82%.

4.2.4. Assay IV

The same strategy from the previous assay was used. The only changes made were the use of a second impeller to the bioreactor's rotor shaft and increasing air supply even further (5 $L.h^{-1}$), in order to avoid limiting yeast growth and reserve products accumulation due to oxygen deficiency.

Figure 15 shows the profiles of the biomass concentration, optical density, biomass productivity, the natural logarithm of the biomass, DO, stirring rate, residual glucose and nitrogen concentrations, fatty acid percentage and productivity, TC concentration and productivity for this assay.

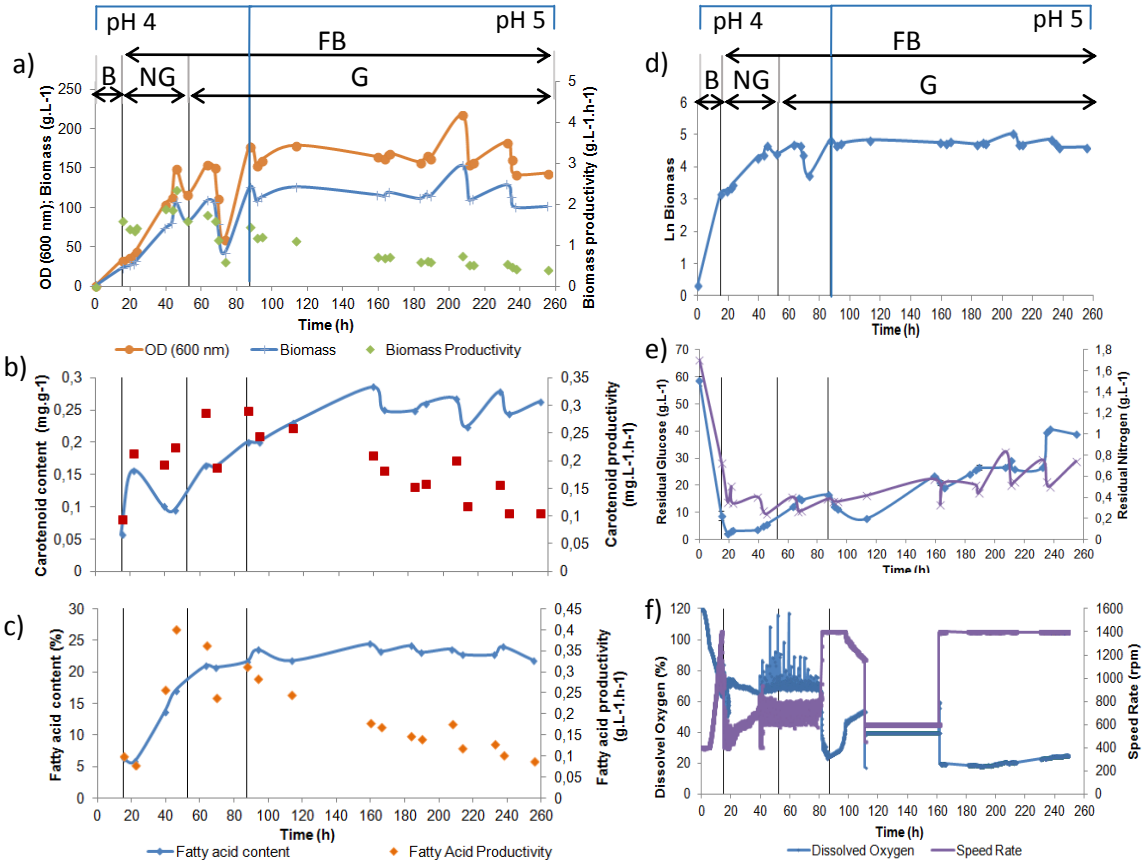

Figure 15. *R. toruloides* yeast growth in a fed-batch system with addition of a nutrient solution with glucose, yeast extract and magnesium sulphate, and concentrated glucose solution via a peristaltic pump, at pH 4.0 and 5.0 (Assay IV): **a)** Optical density (OD), yeast biomass concentration in $g.L^{-1}$ and productivity in $g.L^{-1}.h^{-1}$. The OD and biomass concentration values are the average of at least two replicates with a standard deviation of less than 10% (n = 2); **b)** TC concentration in $mg.L^{-1}$ and carotenoids productivity in $mg.L^{-1}.h^{-1}$; **c)** Fatty acid percentage and fatty acid productivity in $g.L^{-1}h^{-1}$. Fatty acid data represent the mean of four determinations (two independent samples injected twice with a standard deviation of less than 10% (n = 4); **d)** Natural logarithm profile; **e)** Residual glucose and nitrogen concentrations profiles in $g.L^{-1}$. Values are the average of the replicates with a standard deviation of less than 10% (n = 2); **f)** DO and bioreactor speed rate in rpm.
B = batch phase; FB = fed-batch phase; NG = nutrients with glucose solution; G = concentrated (600 $g.L^{-1}$) glucose solution.

The specific growth rate for the NG addition phase was 0.05 h^{-1} (R^2 = 0.99) (Figure 14d). Addition of solution NG began at t = 15 h and solution G was added to the bioreactor at t = 52.5 h. The culture medium pH was changed from 4.0 to 5.0 at t = 87 h. Air inflow was increased to 5 $L.h^{-1}$ at t = 43.5 h (not shown)

The culture entered the stationary phase at t = 87 h with a biomass concentration of 126.14 $g.L^{-1}$ corresponding to 178 OD and a biomass productivity of 1.45 $gL^{-1}.h^{-1}$ (Figure 14a).

Residual nitrogen levels decreased from 1.70 $g.L^{-1}$ to 0.36 $g.L^{-1}$ up to t = 20.00 h, oscillating during the addition of NG and G solutions until the pH was changed to 5.0 when it started to increase and oscillating again at the end of the assay (Figure 14e). Once more, this increase was due to inaccurate ammonia titrations when determining residual nitrogen.

Residual glucose levels decreased from 58.54 $g.L^{-1}$ to 2.08 $g.L^{-1}$ during the batch phase (Figure 14e). At the end of solution NG addition period, levels started rising until the pH change indicating that the culture reached the stationary phase. Then it decreased until t = 113 h increasing afterwards until the end of the assay when it reached levels close to 40 $g.L^{-1}$ (Figure 14e).

The use of two Rushton impellers gave positive results. Although DO readings reached percentages below 40% from t = 81.84 h to t = 97 h and t ≥ 161.55 h, the overall percentages were much higher and were maintained for much longer periods when compared to the previous assays (Figure 14f). The effects of a higher oxygen availability are evident by the higher biomass concentration (154.21 $g.L^{-1}$ at t = 207 h) (Figure 14a), biomass productivity (2.35 $g.L^{-1}.h^{-1}$ at t = 45.5 h) (Figure 14a), fatty acids productivity (0.40 $g.L^{-1}.h^{-1}$ at t = 45.5 h) (Figure 14c), carotenoids productivity (0.29 $g.L^{-1}.h^{-1}$ at t = 87 h) (Figure 14b) and TC content (0.29 $mg.g^{-1}$ at t = 157 h) attained in this experiment (Figure 14b).

Figure 16 shows the fatty acids composition obtained during this assay.

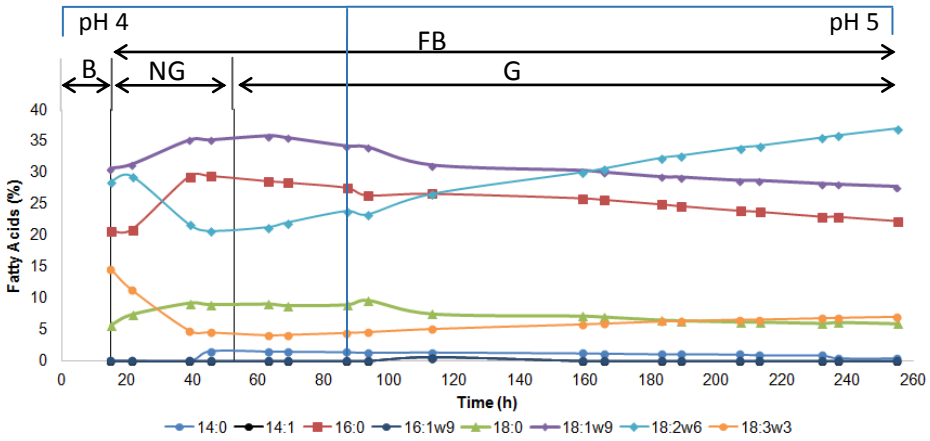

Figure 16. Fatty acid composition percentage obtained in assay IV for *R. toruloides* with addition of nutrients with glucose and concentrated glucose solutions via peristaltic pump, at pH 4.0 – 5.0. The data represent the mean of two determinations (two independent samples injected twice) with a standard deviation lower than 10% (n = 4).
B = batch phase; FB = fed-batch phase; NG = nutrients with glucose solution; G = concentrated (600 $g.L^{-1}$) glucose solution.

Once more, oleic (18:1ω9), palmitic (16:0) and linoleic (18:2ω6) acids were dominant.

Oleic acid (18:1ω9) percentages are in the range published by Sawangkeaw *et al*. (2013) [**78**] for *R. toruloides* (18:1ω9: 18-42%). Palmitic acid (16:0) percentages are above the range given by these authors (16:0: 13-16%). Linoleic acid (18:2ω6) percentages are in the range of published values (18:2ω6: 15-29%) with the exception of t ≥ 160 h. Stearic acid (18:0) percentages are in the range of published values.

At the end of the assay (t = 255 h), linoleic acid (18:2ω6) represented the majority of total fatty acids with 36.89%, followed by oleic (18:1ω9) and palmitic (16:0) acids with 27.65% and 22.21%, respectively.

Oleic acid (18:1ω9) percentage increased until t = 63 h, from 30% to 35.76%, then decreasing up to t = 255 h to 27.65%.

Palmitic acid (16:0) increased until t = 39 h from 20.66% to 29.28%, decreasing afterwards until the end of the assay to 22.21%.

Linoleic (18:2ω6) increased slightly up to t = 20 h (from 28.44% to 30%) and then showed the same profile as linolenic acid (18:3ω3), decreasing during the addition of solution NG (from 30% to 20.61% and 14.66% to 4.50%, respectively) and increasing until the end of the assay (to 36.89% and to 6.98%, respectively).

Palmitoleic (16:1ω9) and myristoleic (14:1) acids were both detected in this assay at t = 113 h with very low percentages (0.49% and 0.52%, respectively).

With the exception of t = 15 h, linolenic acid (18:3ω3) remained below 12% and no polyunsaturated fatty acids with four or more double bonds were detected, therefore the

fatty acids profile is in accordance with the requirements imposed by the European standard.

Figure 17 shows the percentage of saturated fatty acids (SFA) monounsaturated fatty acids (MUFA) and polyunsaturated fatty acids (PUFA) for this assay.

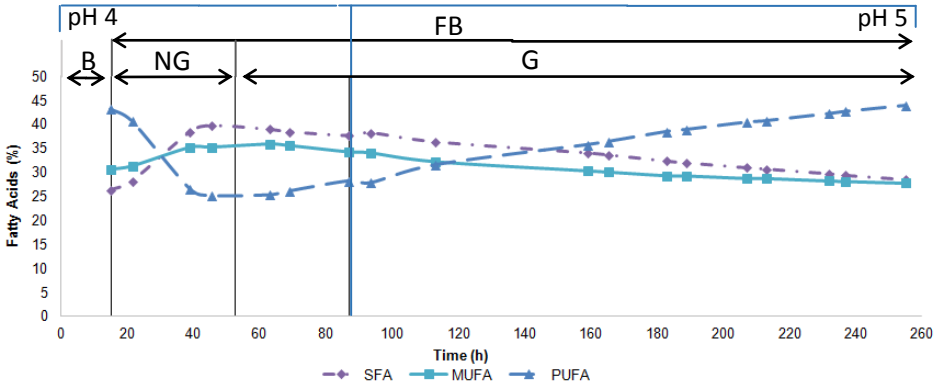

Figure 17. Composition of saturated fatty acids (SFA), monounsaturated fatty acids (MUFA) and polyunsaturated fatty acids (PUFA) obtained in assay IV for *R. toruloides* with addition of NG and G solutions via peristaltic pump, at pH 4.0 - 5.0.
B = batch phase; FB = fed-batch phase; NG = nutrients with glucose solution; G = concentrated (600 $g.L^{-1}$) glucose solution.

PUFA show the highest percentage (43.87%). SFA and MUFA show proximate percentages, with 28.48% and 26.65%, respectively. PUFA have a maximum at t = 15 h with 43.11%, MUFA at t = 63 h with 35.76% and SFA at t = 45.5 h with 39.76%.

SFA and MUFA both increased during the addition of solution NG (from 26.33% to 39.74% and from 30.57% to 35.13%, respectively) and decreased during the addition of the solution G until the end of the assay. PUFA decreased during the addition of solution NG (from 43.11% to 25.11%) and increased until the end of the assay.

4.3. Discussion and comparison between assays

Table 4 shows the summarized results for all assays with *R.toruloides* NCYC 921.

Table 4. Summarized results for assays I, II, II and IV using *R.toruloides* NCYC 921

		Assay I	Assay II	Assay III	Assay IV
Number of turbines		1	1	1	2
pH		5.5	4.0	4.0 – 5.0	4-0 – 5.0
μ (h^{-1})		0.05 (R^2 = 0.99)	0.05 (R^2 = 0.98)	0.05 (R^2 = 0.93)	0.05 (R^2 = 0.99)
Maximum biomass concentration ($g.L^{-1}$)		97.18 (t = 97 h)	119.61 (t = 96.5 h)	128.26 (t = 159 h)	154.21 (t = 207 h)
Maximum biomass productivity ($g.L^{-1}.h^{-1}$)		1.58 (t = 50 h)	1.76 (t = 47 h)	1.94 (t = 44 h)	2.35 (t = 45.5 h)
Maximum fatty acids (% w/w)		27.57 (t = 74 h)	26.19 (t = 117.67 h)	27.88 (t = 183 h)	24.40 (t = 159 h)
Maximum fatty acid productivity ($g.L^{-1}.h^{-1}$)		0.38 (t = 74 h)	0.32 (t = 96.5 h)	0.29 (t = 93.5 h)	0.40 (t = 45.5 h)
Maximum fatty acid concentration ($g.L^{-1}$)		28.12 (t = 74 h)	30.88 (t = 96.5 h)	27.12 (t = 93.5 h)	18.2 (t = 45.5 h)
Maximum carotenoid concentration ($mg.g^{-1}$)		0.28 (t = 144 h)	0.15 (t = 118.5 h)	0.18 (t = 159.5 h)	0.29 (t = 157 h)
Maximum carotenoid concentration ($mg.L^{-1}$)		27.21 (t = 144 h)	17.94 (t = 118.5 h)	23.09 (t = 159.5 h)	44.72 (t = 157 h)
Maximum carotenoid productivity ($g.L^{-1}.h^{-1}$)		0.19 (t = 144 h)	0.12 (t = 118.5 h)	0.16 (t = 120 h)	0.29 (t = 87 h)
Total lipid content (%)		39.42	28.30	39.04	41.07
Average total fatty acid content (%)	**SFA**	39.68	30.75	35.40	33.53
	MUFA	35.99	37.41	33.17	31.28
	PUFA	35.17	31.84	31.43	35.19
European standard requirements		Fulfilled	Fulfilled (except t = 19 h)	Fulfilled	Fulfilled (except t = 15 h)

When comparing the parameters calculated for all four assays, one can conclude that there are two important factors influencing these values: oxygen availability and medium pH.

The pH used in assay II resulted in a 23.08% increase in the maximum biomass concentration and a 10.23% increase in maximum biomass productivity compared to assay I. The maximum biomass concentration obtained for assay II, as well as in assays III and IV, were higher than the concentration reported by Li *et al.* (2007) (106.5 $g.L^{-1}$) using *Rhodosporidium toruloides* Y4 grown in 15 L bioreactors in fed-batch cultivations with glucose as the carbon source [**82**].

Fatty acid and total lipid percentages and carotenoid concentration in assay II were lower than in assay I. The lack of oxygen in the culture may explain this reduction compared to the previous trial. However, even with this limitation, the maximum fatty acid concentration in assay II was higher than the previous assay, possibly due to higher biomass productivity, which is tightly related to fatty acid synthesis [**54**].

The results in assay IV, due to a more efficient oxygen distribution to the culture, are in agreement with those from Saenge *et al.* (2011b) who reported a significant increase in the biomass concentration and lipid production and a slight increase of carotenoid production after increasing the aeration rate in *Rhodotorula glutinis* fed-batch cultures [**83**]. Other authors have also reported the positive effects of aeration on carotenoid content [**84-86**].

However, carotenoid values for assay IV were relatively low compared to the results obtained by Saenge *et al.* (2011a; 2011b) [**32, 83**]. In contrast, the total lipid concentration values obtained by these authors were much lower than the results obtained in all assays. Observing the decrease of the maximum fatty acid percentage and fatty acid concentration in assay IV, it might suggest that fatty acid and carotenoid production are inverse to one another. This can be explained by the fact that fatty acids are, as previously mentioned, a product uniquely associated with the yeast's growth [**54**] while carotenoids are a mixed product (associated with the growth and also produced in the stationary phase, as reserves) [**54, 87**].

Assays I and IV show higher fatty acid productivity than the productivity obtained by Zhao *et al.* (2011) [**88**] for a fed-batch system with intermittent 30 $g.L^{-1}$ glucose feed (0.36 $g.L^{-1}.h^{-1}$). The fatty acid productivity obtained in assay IV was higher than the value reported by the same authors but with continuous 30 $g.L^{-1}$ glucose feed (0.39 $g.L^{-1}.h^{-1}$).

Total lipid content in the biomass for all assays was lower than the percentages given by Wiebe *et al.* (2012) [**89**] when using glucose (48 - 75%) in their nitrogen restricted medium used to cultivate *Rhodosporidium toruloides* in batch and fed-batch cultures in 0.5 L bioreactors at pH 4. With the exception of assay II, total lipid content of yeast

biomass for the other assays are in the range of those observed by Wiebe *et al.* (2012) when using xylose as the carbon source (36 - 45%), and higher than the percentages obtained when using arabinose (15 - 19%) [**89**].

All assays presented fatty acid compositions fulfilling EN 14214 requirements (with the exception of t = 19 h in assay II and t = 15 h in assay IV, with 18:3ω3 percentages above 12%).

Low amounts of PUFA and SFA are required to ensure good quality biodiesel with satisfactory properties [**90**], therefore the fatty acid composition from assay II is the one that guarantees the best biodiesel properties due to its high MUFA content. The higher levels of PUFA in *R. toruloides* oil found in assay IV gives its biodiesel lower oxidative stability [**32**]. However, this is not impeditive to obtain a good quality biodiesel if associated with other oils [**91**].

4.4. Flow Cytometry

In this study we used FC to detect cell viability during the development of all cultivations. This technique also allowed us to quantify the TC content produced by *R. toruloides* (Section 3.8.2.) and monitor cell viability by detecting the integrity of the cytoplasmic membrane and mitochondrial membrane potential (Section 3.8.1.), in real time. Previous subpopulation controls were performed by Freitas *et al.* (2014) for *R. toruloides* [**54**] (Annex II).

Figures 18 to 21 show the sub-populations profiles obtained from the density plots of *R. toruloides* cells double-stained with $DiOC_6(3)$ and PI, harvested during assays I – IV, in different physiological states.

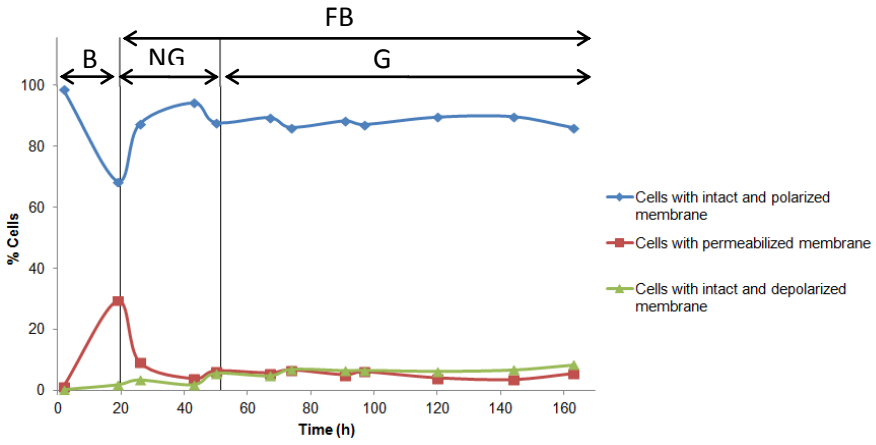

Figure 18. R. *toruloides* cells physiological states analyzed during assay I.
B = batch phase; FB = fed-batch phase; NG = nutrients with glucose solution; G = concentrated (600 $g.L^{-1}$) glucose solution.

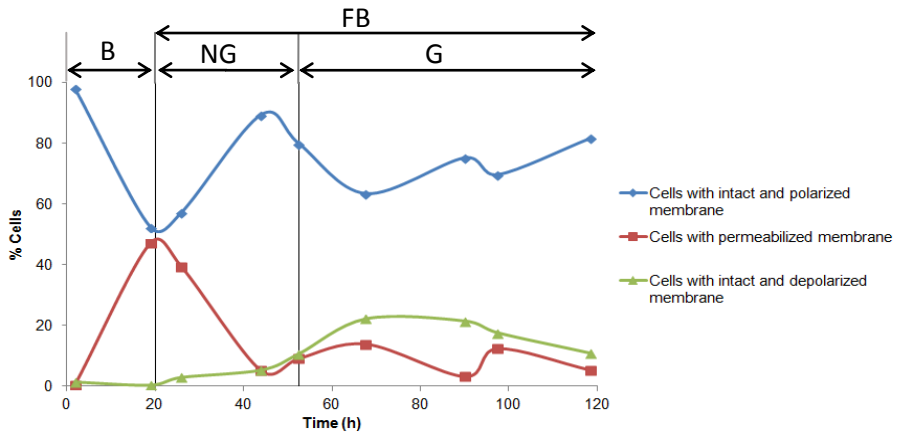

Figure 19. R. *toruloides* cells physiological states analyzed during assay II.
B = batch phase; FB = fed-batch phase; NG = nutrients with glucose solution; G = concentrated (600 $g.L^{-1}$) glucose solution.

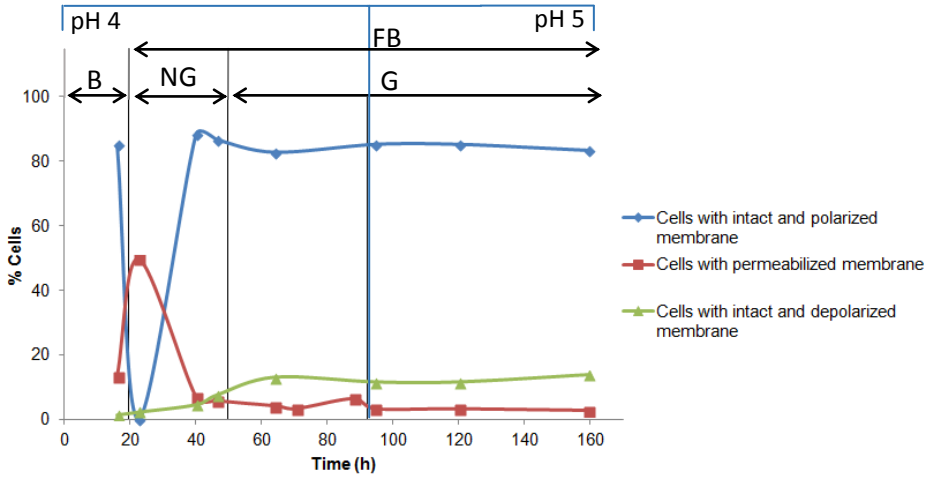

Figure 20. R. *toruloides* cells physiological states analyzed during assay III.
B = batch phase; FB = fed-batch phase; NG = nutrients with glucose solution; G = concentrated (600 $g.L^{-1}$) glucose solution.

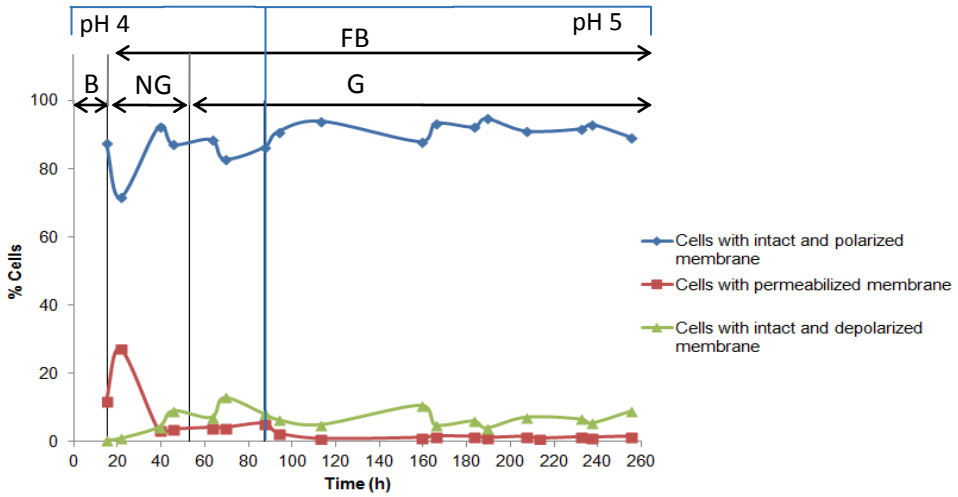

Figure 21. R. *toruloides* cells physiological states analyzed during assay IV.
B = batch phase; FB = fed-batch phase; NG = nutrients with glucose solution; G = concentrated (600 $g.L^{-1}$) glucose solution.

Generally, all assays show an increase in depolarized cells during the batch phase. This increase is attributed to cell stress induced by starvation from the yeast cells' metabolic activity when consuming the glucose present in the pre-cultures at the end of the batch phase.

Particularly in assay I, at the end of the batch phase, the proportion of intact cells with polarized membranes reached 65%, and the proportion of cells with intact and depolarized membranes was 35% (Figure 17). When solution NG was added, the proportion of intact cells with polarized membranes increased and stabilized at values close to 88 % during the G solution feeding period. Intact cells with depolarized membranes remained at around 6% (Figure 17) during the addition of the concentrated glucose solution while cells with permeabilized membranes stayed at very low percentages throughout the whole assay.

Assay II displays the highest percentage of stressed cells and the lowest proportion of intact and polarized cells compared to other assays. The sharp drop in the polarized cells proportion and the simultaneous increase in the depolarized cells proportion at t = 44 h (Figure 18) was coincident with the drop in DO and glucose concentration during this assay (Figure 18).

Assay III presents 49.6% of permeabilized cells at the end of the batch period. The percentage of intact cells with depolarized membrane increased after switching to the concentrated glucose solution, ranging between 12-13.0% until the end of this assay, while the proportion of normal cells remained at about 83% during the feeding period (Figure 19).

Once again, the effects of aeration in assay IV can be seen when looking at the profiles displayed in figure 20, showing the highest percentage of intact and polarized cells out of all assays. In contrast, cells with depolarized membrane and permeabilized membrane remained at very low percentages, the former never exceeding 13% while the latter always remained below 6%.

5. Conclusions and future prospects

This work's aim was to implement a suitable strategy for the improvement of lipids and carotenoids production by the red yeast *Rhodosporidium toruloides* NCYC 921 grown in a fed-batch bench 7L-reactor under various conditions.

Working with a medium pH of 4 gave the highest biomass concentration and biomass productivity compared to our first assay with a medium pH of 5.5. However, as a result of selecting the most suitable pH for high density growth, the production of storage materials was diminished. Failure to predict how much the dissolved oxygen in the

medium would decrease at the time, due to increased cell growth, also contributed to the poor results in this assay, due to oxygen limiting conditions.

Changing the pH medium from 4 to 5 during the stationary phase was successful, as biomass, lipid and carotenoid productivities increased. Still, it was not until we provided more efficient aeration that we observed oxygen was indeed fundamental during the yeast cultivation, giving the highest productivities out of all assays.

FC proved to be an useful tool for monitoring yeast cells near real time, giving us instant quantification of TC as well as observe their physiological states as the cultivation conditions in the bioreactor changed, allowing us to immediately control the entire process to best suit the yeast's needs to ensure the best results. This would have not been possible if we had used time consuming traditional microbiological techniques that would have only given results long after the entire process had ended.

Using FC, we found that mitochondrial activity and integrity of the cytoplasmic membrane of *R. toruloides* cells are affected by lack of nutrients and oxygen.

Having already found a way to improve lipids and carotenoids production, the next step in our work will focus on the process optimization. It is expected that the scale-up step using low-cost industrial by-products such as carob pulp syrup as a carbon source (using a 35 L reactor) will make the process more cost-efficient.

References

1. De Almeida, P., & Silva, P. D. (2011). Timing and future consequences of the peak of oil production. *Futures*, *43*(10), 1044–1055. doi:10.1016/j.futures.2011.07.004

2. Owen, N. a., Inderwildi, O. R., & King, D. a. (2010). The status of conventional world oil reserves—Hype or cause for concern? *Energy Policy*, *38* (8), 4743–4749. doi:10.1016/j.enpol.2010.02.026

3. Höök, M., & Tang, X. (2013). Depletion of fossil fuels and anthropogenic climate change—A review. *Energy Policy*, *52*, 797–809. doi:10.1016/j.enpol.2012.10.046

4. Mohr, S. H., Wang, J., Ellem, G., Ward, J., & Giurco, D. (2015). Projection of world fossil fuels by country. *Fuel*, *141*, 120–135. doi:10.1016/j.fuel.2014.10.030

5. Maggio, G., & Cacciola, G. (2012). When will oil, natural gas, and coal peak? *Fuel*, *98*(2012), 111–123. doi:10.1016/j.fuel.2012.03.021

6. Nigam, P. S., & Singh, A. (2011). Production of liquid biofuels from renewable resources. *Progress in Energy and Combustion Science*, *37*(1), 52–68. doi:10.1016/j.pecs.2010.01.003

7. IEA. International energy outlook; 2013.

8. BP. BP energy outlook 2035. January 2014. Tech. rep; 2014.

9. IPCC. Climate change 2013: the physical science basis. Contribution of working group I to the fifth assessment report of the intergovernmental panel on climate change. Cambridge (UK), NY (USA): Cambridge University Press; 2013

10. Capellán-Pérez, I., Mediavilla, M., de Castro, C., Carpintero, Ó., & Miguel, L. J. (2014). Fossil fuel depletion and socio-economic scenarios: An integrated approach. *Energy*, *77*, 641–666. doi:10.1016/j.energy.2014.09.063

11. Verbruggen, A., & Al Marchohi, M. (2010). Views on PO and its relation to climate change policy. *Energy Policy*, *38*(10), 5572–5581. doi:10.1016/j.enpol.2010.05.002

12. Malthus, T. (1798). An Essay on the Principle of Population. Penguin Classics, London, England, ISBN: 978-0140432060, p. 304.

13. Verhulst, P.F. (1838). Notice sur la loi que la population suit dans son accroisse- ment. Correspondence Mathematique et Physique 10, 113–121

14. Jevons, W.S. (1856). The Coal Question: An Inquiry Concerning the Progress of the Nation, and the Probable Exhaustion of Our Coal-Mines. Augustus M Kelley Pubs, London, England, ISBN: 978-0678001073.

15. Hubbert, M.K. (1956). Nuclear energy and the fossil fuels. Shell Development Company, Houston, Texas, Publication No. 95, pp. 40.

16. Bardi, U. (2009). PO: The four stages of a new idea. *Energy*, *34*(3), 323–326. doi:10.1016/j.energy.2008.08.015

17. Sorrell, S., Speirs, J., Bentley, R., Brandt, A., & Miller, R. (2010). Global oil depletion: A review of the evidence. *Energy Policy*, *38*(9), 5290–5295. doi:10.1016/j.enpol.2010.04.046

18. Campbell, C., & Laherrère, J. (1998). The end of cheap oil. Scientific American, (March).

19. Ribeiro, L. a., da Silva, P. P., Mata, T. M., & Martins, A. a. (2015). Prospects of using microalgae for biofuels production: Results of a Delphi study. *Renewable Energy*, *75*, 799–804. doi:10.1016/j.renene.2014.10.065

20. Azad, a. K., Rasul, M. G., Khan, M. M. K., Sharma, S. C., & Hazrat, M. a. (2015). Prospect of biofuels as an alternative transport fuel in Australia. *Renewable and Sustainable Energy Reviews*, *43*, 331–351. doi:10.1016/j.rser.2014.11.047

21. Rashid, N., Ur Rehman, M. S., Sadiq, M., Mahmood, T., & Han, J.-I. (2014). Current status, issues and developments in microalgae derived biodiesel production. *Renewable and Sustainable Energy Reviews*, *40*, 760–778. doi:10.1016/j.rser.2014.07.104

22. Lee, R. a., & Lavoie, J.-M. (2013). From first- to third-generation biofuels: Challenges of producing a commodity from a biomass of increasing complexity. *Animal Frontiers*, *3*(2), 6–11. doi:10.2527/af.2013-0010

23. Dragone, G., Fernandes, B., Vicente, A. A., & Teixeira, J. A. (2010). Third generation biofuels from microalgae, 1355–1366.

24. Tanner, S. (2009). Biofuels of the Third Generation Do Microalgae Solve the Energy Problem ?

25. André Cremonez, P., Feroldi, M., Cézar Nadaleti, W., de Rossi, E., Feiden, A., de Camargo, M. P., Cremonez, Filipe Eliazar, Klajn, F. F. (2015). Biodiesel production in Brazil: Current scenario and perspectives. *Renewable and Sustainable Energy Reviews*, *42*, 415–428. doi:10.1016/j.rser.2014.10.004

26. Ribeiro, L. a., da Silva, P. P., Mata, T. M., & Martins, A. a. (2015). Prospects of using microalgae for biofuels production: Results of a Delphi study. *Renewable Energy*, *75*, 799–804. doi:10.1016/j.renene.2014.10.065

27. Arifin, Y., Tanudjaja, E., Dimyati, A., & Pinontoan, R. (2014). A Second Generation Biofuel from Cellulosic Agricultural By-product Fermentation Using *Clostridium* Species for Electricity Generation. *Energy Procedia*, *47*, 310–315. doi:10.1016/j.egypro.2014.01.230

28. Galadima, A., & Muraza, O. (2014). Biodiesel production from algae by using heterogeneous catalysts: A critical review. *Energy*, 0–11. doi:10.1016/j.energy.2014.06.018

29. Rashid, N., Ur Rehman, M. S., Sadiq, M., Mahmood, T., & Han, J.-I. (2014). Current status, issues and developments in microalgae derived biodiesel production. *Renewable and Sustainable Energy Reviews*, *40*, 760–778. doi:10.1016/j.rser.2014.07.104

30. Meng, X., Yang, J., Xu, X., Zhang, L., Nie, Q., & Xian, M. (2009). Biodiesel production from oleaginous microorganisms. *Renewable Energy*, *34*(1), 1–5. doi:10.1016/j.renene.2008.04.014

31. Sitepu, I. R., Garay, L. a, Sestric, R., Levin, D., Block, D. E., German, J. B., & Boundy-Mills, K. L. (2014). Oleaginous yeasts for biodiesel: current and future trends in biology and production. *Biotechnology Advances*, *32*(7), 1336–60. doi:10.1016/j.biotechadv.2014.08.003

32. Saenge, C., Cheirsilp, B., Suksaroge, T. T., & Bourtoom, T. (2011). Efficient concomitant production of lipids and carotenoids by oleaginous red yeast *Rhodotorula glutinis* cultured in palm oil mill effluent and application of lipids for biodiesel production. *Biotechnology and Bioprocess Engineering*, *16*(1), 23–33. doi:10.1007/s12257-010-0083-2

33. Venkata Subhash, G., & Venkata Mohan, S. (2014). Lipid accumulation for biodiesel production by oleaginous fungus Aspergillus awamori: Influence of critical factors. *Fuel*, *116*, 509–515. doi:10.1016/j.fuel.2013.08.035

34. Huang, C., Chen, X., Xiong, L., Chen, X., Ma, L., & Chen, Y. (2013). Single cell oil production from low-cost substrates: the possibility and potential of its industrialization. *Biotechnology Advances*, *31*(2), 129–39. doi:10.1016/j.biotechadv.2012.08.010

35. Karatay, S. E., & Dönmez, G. (2010). Improving the lipid accumulation properties of the yeast cells for biodiesel production using molasses. *Bioresource Technology*, *101*(20), 7988–90. doi:10.1016/j.biortech.2010.05.054

36. Vicente, G., Bautista, L. F., Rodríguez, R., Gutiérrez, F. J., Sádaba, I., Ruiz-Vázquez, R. M., Torres-Martínez, S., Garre, V. (2009). Biodiesel production from biomass of an oleaginous fungus. *Biochemical Engineering Journal*, *48*(1), 22–27. doi:10.1016/j.bej.2009.07.014

37. Leite, G. B., Abdelaziz, A. E. M., & Hallenbeck, P. C. (2013). Algal biofuels: challenges and opportunities. *Bioresource Technology*, *145*, 134–41. doi:10.1016/j.biortech.2013.02.007

38. Da Silva, T. L., Feijão, D., & Reis, A. (2010). Using multi-parameter flow cytometry to monitor the yeast Rhodotorula glutinis CCMI 145 batch growth and oil production towards biodiesel. *Applied Biochemistry and Biotechnology*, *162*(8), 2166–76. doi:10.1007/s12010-010-8991-3

39. Liu J, Huang J, Sun Z, Zhong Y, Jiang Y, Chen F (2011). Differential lipid and fatty acid profiles of photoautotrophic and heterotrophic *Chlorella zofingiensis*: Assessment of algal oils for biodiesel production. Bioresour Technol;102:106–10

40. Da Silva, T. L., Roseiro, J. C., & Reis, A. (2012). Applications and perspectives of multi-parameter flow cytometry to microbial biofuels production processes. *Trends in Biotechnology*, *30*(4), 225–32. doi:10.1016/j.tibtech.2011.11.005

41. Beopoulos, A., Nicaud, J.-M., & Gaillardin, C. (2011). An overview of lipid metabolism in yeasts and its impact on biotechnological processes. *Applied Microbiology and Biotechnology*, *90*(4), 1193–206. doi:10.1007/s00253-011-3212-8

42. Fresenius, J. B. G. W. (1850): *Beiträge zur Mykologie* 1

43. Harrison, F. C. (1928): *Proceedings and Transactions of the Royal Society of Canada, 3rd Series 22*

44. Lodder, J. (1934): *Die anaskosporogenen Hefen, I. Hälfte. Verhandelingen der Koninklijke Nederlandsche Akademie van Wetenschappen* 32.

45. *The Yeasts: A Taxonomic Study.* J. Lodder and N. J. W. Kreger-Van Rij. Amsterdam: North-Holland Pub.; New York: Interscience, 1952. 713 pp.

46. *The Yeasts: A Taxonomic Study, 2nd* Edition. J. Lodder. North-Holland Publishing Company, Amsterdam, 1970. 1385 pp.

47. Banno, I. (1963). Preliminary report on cell conjugation and mycelial stage in *Rhodotorula* yeasts.- J. Gen. Appl. Microbiol. (Tokyo) 9:249-251.

48. Banno, I. (1967). Studies on the sexuality of *Rhodotorula*. -- J. Gen. Appl. Microbiol. 13: 167-196.

49. Moore, R. T., & Some, R. T. (1972). Some ultrastructural features of Rhodosporidium toruloides Banno, *38*, 417–435.

50. Weijman ACM, Rodrigues de Miranda L (1983). Xylose distribution within and taxonomy of the genera Bullera and Sporobolomyces. Antonie Van Leeuwenhoek; 49:559-562

51. Hernández-Almanza, A., Cesar Montanez, J., Aguilar-González, M. a., Martínez-Ávila, C., Rodríguez-Herrera, R., & Aguilar, C. N. (2014). *Rhodotorula glutinis* as source of pigments and metabolites for food industry. *Food Bioscience*, *5*, 64–72. doi:10.1016/j.fbio.2013.11.007

52. Parreira (2014), "Otimização do processo de produção de lípidos e carotenóides a partir da biomassa da levedura *Rhodotorula glutinis* NRRL Y-1091," Dissertação para obtenção do grau de mestre em Engenharia Alimentar, Universidade de Lisboa, Instituto Superior de Agronomia.

53. *"Rhodotorula Glutinis*." [Online]. Available: http://eol.org/pages/997332/overview [Accessed: 28-December-2014]

54. Freitas, C., Nobre, B., Gouveia, L., Roseiro, J., Reis, A., & Lopes, T. (2014). New at-line flow cytometric protocols for determining carotenoid content and cell viability during Rhodosporidium toruloides NCYC 921 batch growth. *Process Biochemistry*, (49), 554–562.

55. Freitas, C., Parreira, T. M., Roseiro, J., Reis, A., & da Silva, T. L. (2014). Selecting low-cost carbon sources for carotenoid and lipid production by the pink yeast Rhodosporidium toruloides NCYC 921 using flow cytometry. *Bioresource Technology*, *158*, 355–9. doi:10.1016/j.biortech.2014.02.071

56. Jagannadham, M. V. (1999). The structure of carotenoids, 5347.

57. Stahl, W., & Sies, H. (2003). Antioxidant activity of carotenoids. *Molecular Aspects of Medicine*, *24*(6), 345–351. doi:10.1016/S0098-2997(03)00030-X

58. Rock, C. L. (1997). Carotenoids: Biology and treatment. *Pharmacology & Therapeutics*, *75*(3), 185–197. doi:10.1016/S0163-7258(97)00054-5

59. Von Lintig, J., & Sies, H. (2013). Carotenoids. *Archives of Biochemistry and Biophysics*, *539*(2), 99–101. doi:10.1016/j.abb.2013.09.014

60. Rao, a V, & Rao, L. G. (2007). Carotenoids and human health. *Pharmacological Research : The Official Journal of the Italian Pharmacological Society*, *55*(3), 207–16. doi:10.1016/j.phrs.2007.01.012

61. Nishino, H., Murakoshi, M., Tokuda, H., & Satomi, Y. (2009). Cancer prevention by carotenoids. *Archives of Biochemistry and Biophysics*, *483*(2), 165–8. doi:10.1016/j.abb.2008.09.011

62. Woodside, J. V, McGrath, A. J., Lyner, N., & McKinley, M. C. (2014). Carotenoids and health in older people. *Maturitas*. doi:10.1016/j.maturitas.2014.10.012

63. Frengova, G. I., & Beshkova, D. M. (2009). Carotenoids from *Rhodotorula* and *Phaffia*: yeasts of biotechnological importance. *Journal of Industrial Microbiology & Biotechnology*, *36*(2), 163–80. doi:10.1007/s10295-008-0492-9

64. Aksu, Z., & Eren, A. T. (2007). Production of carotenoids by the isolated yeast of *Rhodotorula glutinis*. *Biochemical Engineering Journal*, *35*(2), 107–113. doi:10.1016/j.bej.2007.01.004

65. Cutzu, R., Clemente, A., Reis, A., Nobre, B., Mannazzu, I., Roseiro, J., & Lopes da Silva, T. (2013). Assessment of β-carotene content, cell physiology and morphology of the yellow yeast Rhodotorula glutinis mutant 400A15 using flow cytometry. *Journal of Industrial Microbiology & Biotechnology*, *40*(8), 865–75. doi:10.1007/s10295-013-1278-2

66. Krinsky, N. I. (2001). Carotenoids as antioxidants. *Nutrition*, *17*(10), 815–817. doi:10.1016/S0899-9007(01)00651-7

67. Vílchez, C., Forján, E., Cuaresma, M., Bédmar, F., Garbayo, I., & Vega, J. M. (2011). Marine carotenoids: biological functions and commercial applications. *Marine Drugs*, *9*(3), 319–33. doi:10.3390/md9030319

68. Moliné, M., Libkind, D., & Broock, M. Van. (2012). Microbial Carotenoids From Fungi, *898*, 275–283. doi:10.1007/978-1-61779-918-1

69. J. G. Pan, M. Y. Kwak, and J. S. Rhee, “High density cell culture of Rhodotorula glutinis using oxygen-enriched air,” *Biotechnol. Lett.*, vol. 8, no. 10, pp. 715–718, 1986.

70. Miller, G. (1959). Use of dinitrosalicylic acid reagent for determination of reducing sugar. *Analytical Chemistry*, (lll).

71. Kjeldahl, J. (1883). Neue methode zur bestimmung des stickstoffs in organischen körpern. *Fresenius’ Journal of Analytical Chemistry*, 366–382.

72. Lepage G, Roy CC (1986).J Lipid Res. Jan; 27(1):114-20. Direct transesterification of all classes of lipids in a one-step reaction.

73. Cohen, Z. (1988). EFFECT OF ENVIRONMENTAL CONDITIONS ON FATTY ACID COMPOSITION OF THE RED ALGA PORPHYRIDIUM CRUENTUM CORRELATION TO GROWTH RATE, *J. Phycol.* 24 *332*, 328–332.

74. ISO 659-1998, International Organization for Standardization; Oilseed – Determination of oil content

75. Amor, K. B., Breeuwer, P., Verbaarschot, P., Rombouts, F. M., Akkermans, a. D. L., De Vos, W. M., & Abee, T. (2002). Multiparametric Flow Cytometry and Cell Sorting for the Assessment of Viable, Injured, and Dead Bifidobacterium Cells during Bile Salt Stress. *Applied and Environmental Microbiology*, *68*(11), 5209–5216. doi:10.1128/AEM.68.11.5209-5216.2002

76. Jones, K. H., & Senft, J. a. (1985). An improved method to determine cell viability by simultaneous staining with fluorescein diacetate-propidium iodide. *Journal of Histochemistry & Cytochemistry*, *33*(1), 77–79. doi:10.1177/33.1.2578146.

77. Sauch, J. F., Flanigan, D., Galvin, M. L., Berman, D., & Jakubowskil, W. (1991). Propidium Iodide Indicator of Giardia Cyst Viability, *57*(11), 3243–3247.

78. R. Sawangkeaw and S. Ngamprasertsith (2013) “A review of lipid-based biomasses as feedstocks for biofuels production” *Renew. Sustain. Energy Rev.*, vol. 25, pp. 97–108.

79. “European Standard EN 1421”, 2003.

80. Chopra, A., Tewari, a. K., Vatsala, S., Kumar, R., Sarpal, a. S., & Basu, B. (2011). Determination of Polyunsaturated Fatty Esters (PUFA) in Biodiesel by GC/GC–MS and 1H-NMR Techniques. *Journal of the American Oil Chemists' Society*, *88*(9), 1285–1296. doi:10.1007/s11746-011-1795-y

81. Jeennor, S. (2006). Comparative fatty acid profiling of *Mucor rouxii* under different stress conditions. *FEMS*, *259*(1), 60–6. doi:10.1111/j.1574-6968.2006.00242.x

82. Y. Li, Z. Kent, and F. Bai (2007), “High-density cultivation of oleaginous yeast *Rhodosporidium toruloides* Y4 in fed-batch culture,” vol. 41, pp. 312–317.

83. Saenge, C., Cheirsilp, B., Suksaroge, T. T., & Bourtoom, T. (2011). Potential use of oleaginous red yeast *Rhodotorula glutinis* for the bioconversion of crude glycerol from biodiesel plant to lipids and carotenoids. *Process Biochemistry*, *46*(1), 210–218. doi:10.1016/j.procbio.2010.08.009

84. Simova, E. D., Frengova, G. I., & Beshkova, D. M. (2003). Effect of Aeration on the Production of Carotenoid Pigments by *Rhodotorula rubra-lactobacillus casei* Subsp. casei Co-Cultures in Whey Ultrafiltrate. *Zeitschrift Für Naturforschung C*, *58*(3-4). doi:10.1515/znc-2003-3-415

85. Davoli, P., Mierau, V., & Weber, R. W. S. (2004). Carotenoids and Fatty Acids in Red Yeasts *Sporobolomyces roseus* and *Rhodotorula glutinis*. *Applied Biochemistry and Microbiology*, *40*(4), 392–397. doi:10.1023/B:ABIM.0000033917.57177.f2

86. Aksu, Z., & Eren, a. T. (2005). Carotenoids production by the yeast *Rhodotorula mucilaginosa*: Use of agricultural wastes as a carbon source. *Process Biochemistry*, *40*(9), 2985–2991. doi:10.1016/j.procbio.2005.01.011

87. Somashekar, D., & Joseph, R. (2000). Inverse relationship between carotenoid and lipid formation in *Rhodotorula gracilis* according to the C/N ratio of the growth medium. *World Journal of Microbiology and Biotechnology*, 491–493.

88. Zhao, X., Hu, C., Wu, S., Shen, H., & Zhao, Z. K. (2010). Lipid production by *Rhodosporidium toruloides* Y4 using different substrate feeding strategies. *Journal of Industrial Microbiology & Biotechnology*, *38*(5), 627–632. doi:10.1007/s10295-010-0808-4

89. Wiebe, M. G., Koivuranta, K., Penttilä, M., & Ruohonen, L. (2012). Lipid production in batch and fed-batch cultures of *Rhodosporidium toruloides* from 5 and 6 carbon carbohydrates. *BMC Biotechnology*, *12*, 26. doi:10.1186/1472-6750-12-26

90. Stansell, G. R., Gray, V. M., & Sym, S. D. (2011). Microalgal fatty acid composition: implications for biodiesel quality. *Journal of Applied Phycology*, *24*(4), 791–801. doi:10.1007/s10811-011-9696-x

91. Da Silva, T. L., Reis, A., Medeiros, R., Oliveira, A. C., & Gouveia, L. (2008). Oil Production towards Biofuel from Autotrophic Microalgae Semicontinuous Cultivations Monitorized by Flow Cytometry. *Applied Biochemistry and Biotechnology*, *159*(2), 568–578. doi:10.1007/s12010-008-8443-5

Annex I – List of reagents

Table A1 lists all the chemical reagents used throughout this work.

Table A1. Chemical reagents used throughout all experimental works. A – assays; CE – carotenoids extraction; CM – culture medium; FC – flow cytometry; HPLC – high performance liquid chromatography; NG – nutrients + glucose solution; RN – residual nitrogen; RS – residual sugars; TL – total lipids; TR – transesterification reaction

Name	MM ($g.mol^{-1}$)	Chemical formula	Purity (%)	Brand	Usage
3,3′-dihexyloxacarbocyanine iodide [$DiOC_6(3)$]	572.23	$C_{29}H_{37}IN_2O_2$	-	Invitrogen	FC
3,5-dinitrosalicylic acid (DNS)	228.12	$C_7H_6O_5.H_2O$	-	Merck	RS
Acetone	58.08	CH_3COCH_3	99.5	Merck	CE;TL
Acetonitrile	41.05	C_2H_3N	-	Carlo Erba	HPLC
Acetyl chloride	78.50	C_2H_3ClO	98.5	Panreac	TR
Aluminum chloride hexahydrate	241.45	$AlCl_3.6H_2O$	97.0	Merck	CM
Ammonium sulphate	132.14	$(NH_4)2SO_4$	99.0	Panreac	CM
Boric acid	61.83	H_3BO_3	99.8	Merck	RN
Calcium chloride dihydrate	147.02	$CaCl_2.2H_2O$	99.5	Merck	CM
Cobalt chloride	129.84	$CoCl_2$	99.0	Fluka	CM
Copper chloride dihydrate	170.48	$CuCl_2.2H_2O$	99.0	Merck	CM
D-Glucose anydrous	180.16	$C_6H_{12}O_6$	99.5	Pronolab	CM; NG; RS
Dimethyl sulfoxide (DMSO)	78.13	C_2H_6OS	-	Riedel-de Haiën	CE;FC
Disodium hydrogen phosphate	141.96	Na_2HPO_4	99.0	Panreac	CM
Ethyl acetate	88.00	$C_4H_8O_2$	-	Carlo Erba	HPLC
Ferrous sulphate heptahydrate	278.02	$FeSO_4.7H_2O$	99.5	Merck	CM
Hydrochloric acid	36.45	HCl	37.0	Merck	A; RN
Magnesium sulphate heptahydrate	246.48	$MgSO_4.7H_2O$	99.5	Merck	CM; NG
Malt Extract Agar Base	-	-	-	Himedia	SM
Manganese sulphate heptahydrate	277.11	MnSO4.7H2O	99.0	-	CM
Methanol	32.04	CH_3OH	99.8	Merck	HPLC; TR; TL
Methyl red	269.30	$C_{15}H_{15}N_3O_2$	-	-	RN
Methylene blue	319.85	$C_{16}H_{18}N_3SCl$	-	-	RN
n-heptane	100.21	C_7H_{16}	99.0	Merck	TR
n-hexane	86.18	C_6H_{14}	99.5	Fisher Chemical	CE; TL
Petroleum ether (40^0C-60^0C)	-	$(CH_3)_3COCH_3$	-	Fisher Chemical	CE
Petroleum ether (80^0C-100^0C)	-	$(CH_3)_3COCH_3$	-	Fisher Chemical	TR
Polypropylene glycol (PPG)	-	-	-	Prolab	A
Potassium dihydrogen phosphate	136.09	KH_2PO_4	99.0	Panreac	CM
Potassium sodium tartarate	282.23	$C_4H_4KNaO_6.4H_2O$	99.0	Panreac	RG
Propidium iodide (PI)	668.4	$C_{27}H_{34}I_2N_4$	-	Invitrogen	FC

Sodium chloride	58.44	NaCl	99.5	Pronolab	CE
Sodium hydroxide	39.99	NaOH	-	José M. Vaz Pereira, S.A.	A;RN
Sodium molybdate dihydrate	241.95	$Na_2MoO_4.2H_2O$	99.5	Merck	CM
Sodium sulphate anydrous	142.04	Na_2SO_4	99.0	Merck	RT, EC
Stearic acid	284.48	$C_{18}H_{36}O_2$	-	-	RN
Sulfuric acid	98.08	H_2SO_4	95.0-97.0	Merck	RN
Triethylamine (TEA)	101.10	$N(CH_2CH_3)_3$	89.5	Panreac	HPLC
Yeast extract	-	-	-	BD	CM; NG
Zinc sulphate heptahydrate	287.55	$ZnSO_4.7H_2O$	99.5	M&B	CM

Annex II – Cell viability controls

Figure A2 shows the flow cytometric controls for *R. toruloides* subpopulation identification.

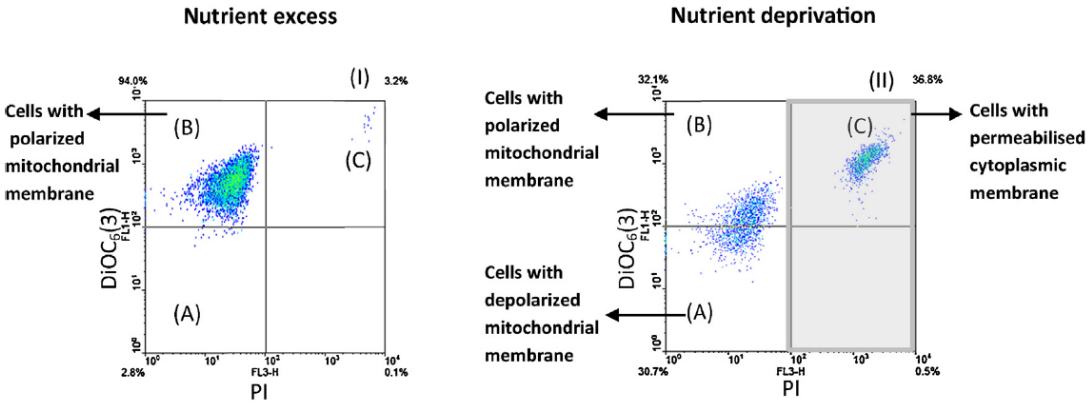

Figure A2. Flow cytometric controls for *R. toruloides* cells stained with PI and $DiOC_6(3)$. Density plot (I) represent yeast cells grown under nutrient excess and density plot (II) stands for stressed cells due to starvation. Gray squares correspond to yeast cells stained with PI. Subpopulation A [$DiOC_6(3)^-$ PI^-] corresponds to cells with intact cytoplasmic membrane, but with depolarized mitochondrial membrane; Subpopulation B [$DiOC_6(3)^+$ PI^-] corresponds to cells with an intact cytoplasmic membrane and polarized mitochondrial membrane; subpopulation C [$DiOC_6(3)^+$ PI^+] shows the permeabilized yeast cells.(Adapted from Freitas *et al.* (2014) [**54**])

These controls allowed us to identify *R. toruloides* physiological states throughout assays I, II, III and IV.